A Dynamic Stochastic Network Model of The Unsecured Interbank Lending Market*

Falk Bräuning[a,c] and Francisco Blasques[a,b,c] and Iman van Lelyveld[d]

[(a)]Department of Econometrics, VU University Amsterdam

[(b)]Department of Finance, VU University Amsterdam

[(c)]Tinbergen Institute [(d)]De Nederlandsche Bank

August 25, 2014

Abstract

We introduce a structural micro-founded dynamic stochastic network model of the unsecured interbank lending market. Banks are profit optimizing agents subject to random liquidity shocks and can engage in costly counterparty search to find suitable trading partners and peer monitoring to reduce counterparty risk uncertainty. We estimate the structural parameters by indirect inference using appropriate network statistics of the Dutch interbank market from 2008 to 2011. The estimated model accurately explains the high sparsity and stability of the lending network. In particular, monitoring of counterparty risk and directed search are key factors in the formation of interbank trading relationships that are associated with improved credit conditions. Moreover, the estimated degree distribution is highly skewed with few very interconnected core banks and many peripheral banks that trade mainly with core banks. We show that shocks to credit risk uncertainty can lead to extended periods of decreased market activity, but reactions are heterogeneous across trading partners. Finally, a larger central bank discount window leads to a more active market through a direct effect and an indirect multiplier effect by increasing banks' monitoring and search efforts.

*Corresponding author: F.Brauning@vu.nl. We thank Henrique Basso, Siem Jan Koopman, Marco van der Leij, Andre Lucas, Albert Menkveld, Gabriel Perez Quiros and Hyun Song Shin for comments. Participants at seminars at De Nederlandsche Bank, Deutsche Bundesbank, Bank of England, Duisenberg School of Finance, 7th annual SoFiE conference, 1st annual IAAE conference, the Banque de France - SoFiE conference on systemic risk and financial regulation, and the GENED workshop on networks in macroeconomics and finance also provided useful feedback. Blasques and Bräuning gratefully acknowledge financial support from the Dutch Science Foundation (NWO) and the SWIFT institute. The opinions expressed in this paper do not necessarily reflect those of De Nederlandsche Bank or the Eurosystem.

1 Introduction

The global financial crisis of 2007-2008 highlighted again the crucial role of interbank lending markets for the financial system and the entire economy. Particularly, after the September 2008 fall of Lehman, dramatic increases in perceived counterparty risk led to severely distressed unsecured interbank markets. As a result, monetary policy implementation was hampered and credit supply to the non-financial sector dropped substantially with adverse consequences for both the financial sector and the real economy. Moreover, the freeze of the Euro area interbank markets within some member countries amplified the sovereign debt crisis in Europe. In order to mitigate these adverse effects, central banks intervened not only by injecting additional liquidity in the banking sector but also by adjusting their monetary policy instruments. As a consequence, central banks became the intermediary for large parts of the money market during the crisis.[1]

This experience further stimulated the debate about the organizational structure of interbank markets. Generally having a central counterparty for the unsecured interbank market reduces contagion effects as credit exposures between banks can no longer give rise to a chain reaction that might bring down large parts of the banking sector, see Allen and Gale (2000). Likewise search frictions that result from asymmetric information about liquidity conditions of other banks are mitigated. On the other hand, with a central counterpart, private information that banks have about the credit risk of other banks is no longer reflected in the price at which banks can obtain liquidity. Thus market discipline is impaired. Moreover, the incentives for banks to acquire and process such information are largely eliminated. However, as Rochet and Tirole (1996) argue, if banks can assess the creditworthiness of other institutions more efficiently than a regulatory authority, a decentralized organization of the interbank market can be optimal.[2] Consequently, in order to assess whether a central counterpart in the unsecured money market is welfare enhancing one has to gauge the extent to which private information about counterparty credit risk and search frictions affect the liquidity allocation in money markets.

Our paper contributes to this debate by introducing and estimating a micro-founded structural dynamic stochastic network model to analyze observed cross-sectional and inter-

[1] See Cœuré (2013) and Heijmans et al. (2014), Video 3 for evidence of the Dutch central bank's role.

[2] Indeed, the ECB highlights the role of monitoring and private information as well: "Specifically, in the unsecured money markets, where loans are uncollateralised, interbank lenders are directly exposed to losses if the interbank loan is not repaid. This gives lenders incentives to collect information about borrowers and to monitor them over the lifetime of the interbank loan [...]. Therefore, unsecured money markets play a key peer monitoring role.", see the speech by Benoît Cœuré, Member of the Executive Board of the ECB, at the Morgan Stanley 16th Annual Global Investment seminar, Tourrettes, Provence, 16 June 2012. `http://www.ecb.europa.eu/press/key/date/2012/html/sp120616.en.html`, retrieved 10/10/2013.

temporal variation in interbank credit availability and conditions. The two key economic drivers of the model outcomes are asymmetric information about counterparty risk and liquidity conditions elsewhere in the market. In particular, we focus on the role of peer monitoring and counterparty search targeted at mitigating credit risk uncertainty and search frictions in a decentralized market. We characterize the bilateral equilibrium interest rates as an increasing function of the outside option for borrowing (given by the central bank's standing facilities), counterparty risk uncertainty and the lender's market power relative to the borrower. Further, we show that the optimal search and monitoring strategy towards all other banks in the network are functions of the expected profitability of trade with each counterparty. Specifically, we find that the optimal dynamic monitoring decision depends on the expected probability of being contacted by distinct borrowers in the future and the expected loan volumes to be traded with these borrowers. Moreover, optimal counterparty search depends on expected volumes and offer rates in each period.

The second novelty of this paper lies in the econometric analysis of the model, in particular the estimation of the structural parameters. In this respect, we go beyond recent interbank research that has focused on theoretical modeling only and does not tackle parameter estimation; see for instance Heider et al. (2009) and Afonso and Lagos (2012), and for more general financial network models Babus (2013). However, the increased availability of granular interbank lending data resulting from payment records makes it feasible to develop a structural economic network model that can be estimated from these data sets. Specifically, we make use of a unique panel of unsecured overnight loans between the largest 50 Dutch banks derived from the TARGET2 payment system records from 2008 to 2011. Crucially, the data contains information on the bilateral volumes and prices of granted loans. Given the dynamic complexity of the model and the presence of latent variables, estimation with classical estimators is largely impossible and we turn to the unifying approach of indirect inference for simulation-based parameter estimation, introduced in Gourieroux et al. (1993) and Smith (1993). Specifically, our indirect inference of the structural parameters is based on a number of descriptive network statistics, e.g. density, reciprocity, clustering and centrality, that have become popular in characterizing the topological structure of interbank markets, see for instance Bech and Atalay (2010). We further complement these network statistics by moment statistics of the data and measures of bilateral lending relationship as in Furfine (1999) and Cocco et al. (2009).

The estimated model is shown to accurately explain several crucial features of the Dutch interbank market. In particular, the estimated parameters reveal that search frictions, counterparty risk uncertainty and peer monitoring are significant factors in matching the structure of the interbank lending network, such as the high sparsity, stability and skewed degree distribution. Moreover, as a result of the interrelation between monitoring and search, some banks form long-term trading relationships that are associated with lower interest rates and improved credit availability. In particular, peer monitoring and search efforts crucially depend on banks' heterogeneous and persistent expectations about bilateral credit availability and conditions. In this respect, our findings highlight the role of banks' heterogeneous liquidity shock distributions (e.g. differences in funding and investment opportunities) in determining bilateral trading opportunities as the fundamental source of lending relationships. In particular, the model estimates imply a tiered network structure with few highly interconnected core banks that intermediate in the market and many sparsely peripheral banks that almost exclusively trade with core banks. Credit risk uncertainty and peer monitoring reinforce this core-periphery structure: large money center banks are more intensively monitored by lenders and they in turn monitor closely their borrowers, leading to both lower bid and offer rates and fueling their role as market intermediaries.

Our dynamic analysis shows that shocks to credit risk uncertainty can bring down lending activity and market volumes for extended periods of time. In particular, banks reduce search and monitoring efforts because interbank lending becomes less profitable relative to the outside options as a result to increased credit risk uncertainty. Feedback loops between monitoring and search amplify this reduction thereby preventing a faster recovery of the market. Moreover, the lending network becomes less connected but more concentrated (larger reciprocity and higher skewness of degree distribution) as banks with extensive relationships stay in the market unlike borrowers that only occasionally access the market. In particular, bank pairs that have low credit risk uncertainty continue to lend to each other and the average rate of granted loans decreases during the crisis period accompanied by larger cross-sectional price dispersion. Furthermore, our policy analysis shows that by increasing the discount window width the ECB fosters interbank lending via directly reducing the attractiveness of the outside options thereby increasing the potential surplus from interbank lending. However, we document a further indirect multiplier effect as increased expected surplus from interbank trading will eventually intensify banks' monitoring and search that in turn further improve credit conditions and availability in the market leading to yet more liquidity and a more efficient market usage.

The paper is structured as follows. Section 2 motivates the paper and discusses the related literature. Section 3 introduces the structural model, defines structural forms, the agents' expectation formation mechanisms and finally obtains a reduced form representation of the structural form. Section 4 provides details on the estimation procedure, discusses the parameter estimates of the model and analyzes their relative fit in terms of various criteria. Finally, Section 5 analyzes the estimated model and studies policy implications. Section 6 concludes.

2 Stylized Facts and Related Literature

In this paper we propose a network model based on credit risk uncertainty and peer monitoring to explain the observed patterns of trading relationships in interbank markets. In particular, we focus on explaining two stylized facts. First, interbank markets exhibit a sparse core-periphery structure whereby a few highly interconnected core banks account for most of the observed trade and many sparsely peripheral banks that almost exclusively trade with core banks.[3] For the Dutch market this structure is visualized in Figure 1. Second, interbank lending is based on stable bilateral trading relationships that are associated with improved access to credit and better access conditions.[4] This characteristic is reflected by the high stability and negative correlation between past bilateral trading and current interest rates in Figure 1. By explaining these two stylized facts our paper relates to several strands of the literature.

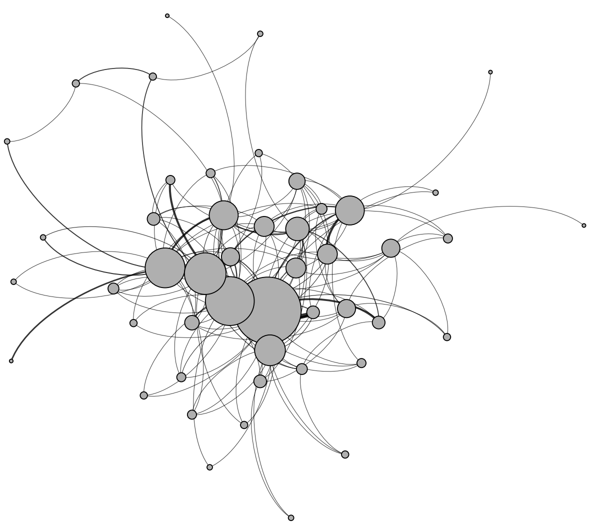

Statistic	Mean	Std
Density	0.0212	0.0068
Stability	0.9818	0.0065
Average degree	1.0380	0.3323
Skewness outdegree	2.8821	1.0346
Skewness indegree	2.4030	0.8787
$\text{Corr}(r_{i,j,t}, l^{rw}_{i,j,t-1})$	-0.0716	0.1573
$\text{Corr}(l_{i,j,t}, l^{rw}_{i,j,t-1})$	0.6439	0.0755

Figure 1: Observed overnight lending network and key statistics. $r_{i,j,t}$ is bilateral interest rate, $l_{i,j,t}$ measures occurrence of overnight loan, $l^{rw}_{i,j,t-1}$ measures past trading intensity.

First, the basic economic driving forces of the proposed interbank lending model are credit

[3]For empirical evidence on the topological structure of interbank markets see, for instance, Soramäki et al. (2007), May et al. (2008) and Bech and Atalay (2010) for the US, Boss et al. (2004) for Austria, Iori et al. (2008) and Lux and Fricke (2012) for Italy, Becher et al. (2008) for the UK, Craig and von Peter (2014) for Germany, and van Lelyveld and in 't Veld (2012) for the Netherlands.

[4]The existence of interbank relationship lending has been documented by, for instance, Furfine (1999), Furfine (2001), Ashcraft and Duffie (2007) and Afonso et al. (2013) for the US, Iori et al. (2008) and Affinito (2011) for Italy, Cocco et al. (2009) for Portugal, Bräuning and Fecht (2012) for Germany.

risk uncertainty, peer monitoring and search frictions. Thereby our paper is related to recent work by Afonso and Lagos (2012) who propose a search model to explain intraday trade dynamics in the spirit of OTC models as in Duffie et al. (2005). Similar, to these authors we also build our dynamic model on bilateral bargaining and search frictions. However, Afonso and Lagos (2012) abstract from the role of bank default which is introduced by Bech and Monnet (2013) in a three-period matching model. Both models do not account for credit risk uncertainty and they do not focus on explaining the network structure of interbank markets. Moreover, assuming a continuum of atomistic agents where the probability of two banks are matched repeatedly is zero, there is no role for the emergence of long-term trading relationships. On the other hand, building on the classical banking model by Diamond and Dybvig (1983), Freixas and Holthausen (2005), Freixas and Jorge (2008) and Heider et al. (2009) have focused on asymmetric information about counterparty risk in competitive and anonymous markets. Hence, these studies abstract from the OTC structure where deals are negotiated on a bilateral basis and credit conditions crucially depend on heterogeneous expectations about counterparty risk and credit conditions. The role of peer monitoring in interbank markets that we consider a key driver has been highlighted by Broecker (1990), Rochet and Tirole (1996) and Furfine (2001).[5]

Second, our paper relates to the growing literature on the formation of financial networks, see Gale and Kariv (2007), Babus (2013), in 't Veld et al. (2014), Vuillemey and Breton (2014) and Farboodi (2014). In particular, Babus (2013) shows that when agents trade risky assets over-the-counter, asymmetric information and costly link formation can endogenously lead to a (undirected) star network with one intermediary. Farboodi (2014) develops a model where banks try to capture intermediation rents that implies a core-periphery structure. Crucially, her model relies on the assumption of differences in investment opportunities, see also in 't Veld et al. (2014). Our model confirms the importance of this type of bank heterogeneity for the emergence of core-periphery structure, but credit risk uncertainty and peer monitoring are the key drivers of persistent bilateral trading relations that reinforce the core-periphery structure. Vuillemey and Breton (2014) propose an endogenous network model of OTC derivative trading that, like ours, contains preferential attachments and bilateral bargaining. Yet, their focus is not on explaining the structure of the observed financial network. As opposed to these studies that are concerned with the emergence of a static network, our

[5] Babus and Kondor (2013) consider information aggregation in OTC markets for a given network structure, where agents infer the asset's value based on other observed market prices and quantities from other transactions. In contrast, in our model of bank-to-bank uncertainty banks engage in bilateral monitoring and do not learn about a counterparties riskiness from other bilateral prices.

paper also analyzes the dynamic behavior of the lending network.[6]

Third, our paper contributes to the scarce literature on parameter estimation of structural network models of the interbank market, and other financial and economic networks. Following Gourieroux et al. (1993) we propose an indirect inference estimation of our structural model using 21 network statistics. Unlike previous merely descriptive empirical studies of interbank networks, e.g. Bech and Atalay (2010), we thereby link the network topology to structural model parameters that are associated with deep economic concepts - credit risk uncertainty, peer monitoring and search frictions. A recent attempt to calibrate a structural network model using simulated method of moments is presented by Gofman (2014). He uses a grid search for three parameters to match five characteristics of the simulated network (including density, maximum degree and the number of intermediaries) with those of the federal funds market as reported by Bech and Atalay (2010).[7] Other recent developments on the econometrics of networks are discussed in Bramoullé and Fortin (2009).

Finally, our findings relate to a large body of studies on the functioning of interbank markets and monetary policy. With respect to the financial crisis, Afonso et al. (2011) show for the US overnight interbank market that counterparty risk concerns plays a larger role in than liquidity hoarding (Acharya and Merrouche (2013)) in explaining the reduction of interbank lending around the days of the Lehman Brothers' bankruptcy. Our finding highlight the role of peer monitoring and credit risk uncertainty for the market structure of interbank markets, see Craig and von Peter (2014), as well as the existence of interbank relationship lending as in Cocco et al. (2009). Our estimated model dynamics show that shocks to counterparty risk uncertainty can bring down lending activity for extended periods, accompanied by increased cross-sectional variation in prices and a more concentrated trading network. Abbassi et al. (2013) provide empirical on the Euro money market during the financial crisis 2007/8. Moreover, our findings that changes in the interest rate corridor lead to direct effects on interbank activity as well as indirect multiplier effects triggered by monitoring and search adjustments, contributes to the debate on the conduct of monetary policy in a corridor system, see Berentsen and Monnet (2008). In particular, our model suggests that increasing the corridor incentivizes peer monitoring and private interbank lending. However, absent a view on the central bank's preferences we cannot make statements on the *optimal* corridor width (cf Bindseil and Jabłecki (2011)).

[6]The effects of the network structure on financial contagion has been studied, for instance, by Georg (2013), Gai et al. (2011), Acemoglu et al. (2013) and Gofman (2014). We do not focus on contagion effects in this paper.

[7]An other first attempts to estimate an information diffusion model using simulated method of moments in the context of income distributions is given by Alatas et al. (2012)

3 The Interbank Network Model

The fundamental driving forces of interbank lending are liquidity shocks that hit banks' payment accounts in their daily business operations (e.g. clients that want to make payments). Banks wish to smooth these shocks by borrowing and lending funds from each other in a decentralized unsecured interbank market or by using the central bank's standing facilities. We model this market as a network consisting of N nodes with a time-varying number of directed links between them. Each node represents a bank and each link represents an interbank loan that is characterized by an loan amount and interest rate. Time periods are indexed by $t \in \mathbb{N}$. Banks in the interbank market are indexed by $i \in \{1, ..., N\}$.

At every period, banks are subject to liquidity shocks and enter the market with the objective to maximize expected discounted interbank market profits by: *(i)* choosing which banks to approach for a transaction; *(ii)* bilaterally negotiating interest rates with other banks willing to trade in the interbank market; and *(iii)* setting monitoring expenditure to gain knowledge about future probabilities of default. As an outside option to interbank lending, banks have unlimited recourse to the central bank's standing facilities (discount window) with deposit rate $\underline{r}$ and borrowing rate $\overline{r}$ with $\overline{r} \geq \underline{r}$.

3.1 Liquidity Shocks

At each period t, every bank enters the market as a potential borrower or lender according to the random vector $\zeta_t = (\zeta_{1,t}, ..., \zeta_{N,t})'$. Each element $\zeta_{i,t} \in \mathbb{R}$, denotes the period t liquidity shock of bank i with $\zeta_{i,t} < 0$ ($\zeta_{i,t} > 0$) being a deficit (surplus). A bank for instance might demand funds because it has an investment opportunity, or it might have funds available as customers deposit money at their accounts.

The distribution of liquidity shocks in the banking system has been identified as one key driver of interbank lending by Allen and Gale (2000) amongst others. We assume that liquidity shocks $\zeta_{i,t}$ are independently and normally distributed with bank specific mean μ_{ζ_i} and variance $\sigma^2_{\zeta_i}$ parameters

$$\zeta_{i,t} \sim \mathcal{N}(\mu_{\zeta_i}, \sigma^2_{\zeta_i}) \quad \text{where} \quad \mu_{\zeta_i} \sim \mathcal{N}(\mu_\mu, \sigma^2_\mu) \quad \text{and} \quad \log \sigma_{\zeta_i} \sim \mathcal{N}(\mu_\sigma, \sigma^2_\sigma),$$

and we allow for correlation between μ_{ζ_i} and $\sigma^2_{\zeta_i}$ through the parameter $\rho_\zeta := corr(\mu_{\zeta_i}, \sigma_{\zeta_i})$. Note that we assume (conditional) independence and normality of liquidity shocks for convenience as it allows us to analytically compute part of the model's solution. This simple type of heterogeneity in the distributions of liquidity shocks allows us to model size effects related to the scale of banks' businesses through larger variances that are drawn from a log-normal distribution. Moreover, it allows us to account for structural liquidity provision or demand by some banks through a nonzero mean $\mu_{\zeta_{i,t}}$.

3.2 Counterparty Risk Uncertainty

Borrowers may default on interbank loans and – due to the unsecured nature of interbank lending – impose losses on lenders. The *true probability of default* of bank j at time t is derived as the tail probability of a random variable $z_{j,t}$ that measures the *true financial distress* of bank j,

$$\mathbb{P}(z_{j,t} > \epsilon).$$

In particular, $z_{j,t}$ is constructed so that bank j is forced into default whenever $z_{j,t}$ takes values above some common time-invariant threshold $\epsilon > 0$. This threshold can be interpreted as either a minimum regulatory requirement or a level that is (seen to be) sufficient to operate in the market. We focus on the case that $z_{j,t}$ is identically and independently distributed for each bank j with $\mathbb{E}(z_{j,t}) = 0$ and $\sigma^2 = \text{Var}(z_{j,t})$, such that there is no heterogeneity in banks' true probability of default.

While counterparty credit risk relates to the riskiness and liquidity of a borrower's assets, asymmetric information about counterparty risk is seen as a major characteristic of financial crises that led to inefficient allocations in money markets, see Heider et al. (2009).[8] Asymmetric information problems arise because counterparty risk assessment is not based on the true but on the *perceived probability of default* that bank i attributes to bank j at time t. This probability is denoted $P_{i,j,t}$ and obtained as the tail probability of a random variable $z_{i,j,t}$ that measures bank i's *perceived financial distress* of bank j. The perceived financial distress $z_{i,j,t}$ contains an added bank-to-bank uncertainty that is modeled by the addition of an independent *perception error* $e_{i,j,t}$ so that,

$$z_{i,j,t} = z_{j,t} + e_{i,j,t}.$$

Note that if the sequence of perception errors $\{e_{i,j,t}\}_{t\in\mathbb{N}}$ is *iid* with $\mathbb{E}(e_{i,j,t}) = 0$ and small variance $\text{Var}(e_{i,j,t}) \approx 0$, then the perceived financial distress is correct on average $\mathbb{E}(z_{i,j,t}) = \mathbb{E}(z_{j,t})$ and added uncertainty is small $\text{Var}(z_{i,j,t}) = \text{Var}(z_{j,t}) + \text{Var}(e_{i,j,t}) \approx \text{Var}(z_{j,t})$. As a

[8] In this respect William Dudley, President and CEO of the Federal Reserve Bank of New York, remarked: «So what happens in a financial crisis? First, the probability distribution representing a creditor's assessment of the value of a financial firm shifts to the left as the financial environment deteriorates [...]. Second, and even more importantly, the dispersion of the probability distribution widens - lenders become more uncertain about the value of the firm. [...] A lack of transparency in the underlying assets will exacerbate this increase in dispersion. ("More Lessons from the Crisis", Nov. 13, 2009)», see `http://www.bis.org/review/r091117a.pdf`

result the perceived probability of default $P_{i,j,t}$ is likely to follow closely the true probability of default $P_{j,t}$.

The time evolution of the distribution of the perception errors is determined by the knowledge that bank i has about the default risk of bank j. This knowledge depends on factors such as the past trading history and, in particular, the monitoring expenditure that bank i allocates to learn about bank j's financial situation, as discussed in more detail in the following section. Specifically, we assume that banks' perception errors have mean zero and variance $\tilde{\sigma}^2_{i,j,t} = \mathrm{Var}(e_{i,j,t})$ that evolves over time according to autoregressive dynamics given by

$$\log \tilde{\sigma}^2_{i,j,t+1} = \alpha_\sigma + \gamma_\sigma \log \tilde{\sigma}^2_{i,j,t} + \beta_\sigma \phi_{i,j,t} + \delta_\sigma u_{i,j,t}. \tag{1}$$

Here $\phi_{i,j,t-1}$ is a function of past bilateral trading intensity and monitoring expenditure that measures the amount of *new information* that bank i collects about the financial situation of bank j in period t, and $u_{i,j,t} \sim \mathcal{N}(0,1)$ is a shock to the counterparty risk uncertainty scaled by $\delta_\sigma > 0$. Moreover we impose that $\beta_\sigma \leq 0$ and hence the added information (weakly) reduces the perception error variance. Note that due to the log specification, $\tilde{\sigma}^2_{i,j,t}$ follows a nonlinear process $\tilde{\sigma}^2_{i,j,t+1} = \xi_{i,j,t}(\phi_{i,j,t}, \tilde{\sigma}^2_{i,j,t}) = \xi(\phi_{i,j,t}, \tilde{\sigma}^2_{i,j,t}, u_{i,j,t})$. Further, $\frac{\partial \xi_{i,j,t}}{\partial \phi_{i,j,t}} < 0$ and $\frac{\partial^2 \xi_{i,j,t}}{\partial \phi^2_{i,j,t}} > 0$ and hence the effect of additional information on the perception error variance is weaker for higher levels of $\phi_{i,j,t-1}$. Thus our model dictates decreasing returns to scale in information gathering.

Since the exact distribution of the perception error $e_{i,j,t}$ is unknown to bank i, every bank is assumed to approximate the tail probability of the extreme event of default by the conservative bound provided by Chebyshev's one-tailed inequality,[9]

$$\mathbb{P}(z_{i,j,t} > \epsilon) \leq \frac{\sigma^2_{i,j,t}}{\sigma^2_{i,j,t} + \epsilon^2} = \frac{\sigma^2 + \tilde{\sigma}^2_{i,j,t}}{\sigma^2 + \tilde{\sigma}^2_{i,j,t} + \epsilon^2} = P_{i,j,t}.$$

Hence, both the true riskiness of a bank as well as the additional uncertainty resulting from the perception error increase the perceived probability of default on which lender banks base their credit risk assessment. Conditional on these bank-specific perceived probabilities of defaults banks bargain about the loan conditions.

[9]Instead of the Chebyshev bound one can assume that the banks use a certain distribution to compute this probability. Then we just have to use the respective CDF here.

3.3 Bargaining and Equilibrium Interest Rates

In the over-the-counter interbank market banks bilaterally negotiate about the loan conditions. Without loss of generality, let bank i be the lender bank ($\zeta_{i,t} > 0$) in the bargaining process and bank j be the borrower bank ($\zeta_{j,t} < 0$). From the point of view of bank i lending funds to bank j at time t is a risky investment with stochastic return

$$R_{i,j,t} = \begin{cases} r_{ijt} & \text{w.p. } 1 - P_{i,j,t} \\ -1 & \text{w.p. } P_{i,j,t}. \end{cases}$$

where we assume that loss given default is 100 percent. We further assume that bank i is risk neutral and maximizes expected lending profit conditional on the perceived probability of default $P_{i,j,t}$. The expected profit per dollar at an equilibrium interest rate $r_{i,j,t}$ is then given by

$$\bar{R}_{i,j,t} = \mathbb{E}_t R_{i,j,t} = (1 - P_{i,j,t})r_{i,j,t} - P_{i,j,t}.$$

For the borrower bank j, the borrowing cost per euro is simply given by the equilibrium interest rate $r_{i,j,t}$ when borrowing from lender bank i.

We follow the standard approach in search models and assume that banks negotiate interest rates bilaterally according to a generalized Nash bargaining, see Afonso and Lagos (2012) for a similar application to interbank markets. Written in terms of excess return relative to the outside options the bilateral equilibrium interest rate then satisfies

$$r_{i,j,t} \in \arg\max_r \left((1 - P_{i,j,t})r - P_{i,j,t} - \underline{r}\right)^\theta \left(\overline{r} - r\right)^{1-\theta},$$

where $\underline{r}$ is the outside option for lenders (e.g., the interest rate for depositing at the central bank), $\overline{r}$ is the the outside option for borrowers (e.g., interest rate for borrowing from the central bank) with $\overline{r} \geq \underline{r}$. The parameter $\theta \in [0, 1]$ denotes the bargaining power of lender i relative to borrower j. As the exchange of funds is voluntary, the bilateral Nash bargaining problem is subject to the participation constraints $r_{i,j,t} \leq \overline{r}$ and $\bar{R}_{i,j,t} \geq \underline{r}$, and hence the interest rate corridor sets an upper and lower bound for the interbank lending rates.[10]

Normalizing $\underline{r} = 0$ and denoting $\overline{r} = r$, the corresponding bilateral equilibrium interest rate between lender i and borrower j is given by

$$r_{i,j,t} = \theta r + (1 - \theta)\frac{P_{i,j,t}}{1 - P_{i,j,t}} \tag{2}$$

[10] In the model all banks have recourse to the outside options at any point in type. Thereby, we abstract for instance from collateral requirements to be eligible for recourse to the standing facilities.

where the last term is a risk premium depending on the perceived probability of default, $P_{i,j,t}$. The minimum interest rate lender i is willing to accept is $r^{min}_{i,j,t} = \frac{P_{i,j,t}}{1-P_{i,j,t}}$ which is obtained from setting $\mathbb{E}_t R_{i,j,t}$ equal to the return of the outside option. Similarly, the borrower will not accept rates higher than $r^{max}_{i,j,t} = r_t$. Note that $\frac{\partial r_{i,j,t}}{\partial P_{i,j,t}} = (1-\theta)/(1-P_{i,j,t})^2 > 0$ and $\frac{\partial^2 r_{i,j,t}}{\partial P^2_{i,j,t}} = 2(1-\theta)/(1-P_{i,j,t})^3 > 0$. It is also easy to see that $\frac{\partial r_{i,j,t}}{\partial \theta} > 0$ for $r_{i,j,t} > r^{min}_{i,j,t}$ such that lenders with more market power are able to obtain higher rates from their borrowers. Further, $\frac{\partial r_{i,j,t}}{\partial r} = \theta > 0$ and hence the bilateral interest rate increases with the outside option for borrowing.

Using the definition of $P_{i,j,t}$ we can rewrite the equilibrium interest rate as a function of the default threshold, the true financial distress variance, and the variance of the perception error as

$$r_{i,j,t} = \theta r + (1-\theta)\frac{\sigma^2 + \tilde{\sigma}^2_{i,j,t}}{\epsilon^2}.$$

Taking the partial derivatives of this function gives $\frac{\partial r_{i,j,t}}{\partial \sigma} = \frac{(1-\theta)2\sigma}{\epsilon^2} > 0$ and $\frac{\partial^2 r_{i,j,t}}{\partial \sigma^2} = \frac{2(1-\theta)}{\epsilon^2} > 0$ and similarly $\frac{\partial r_{i,j,t}}{\partial \tilde{\sigma}_{i,j,t}} = \frac{(1-\theta)2\tilde{\sigma}_{i,j,t}}{\epsilon^2} > 0$ and $\frac{\partial^2 r_{i,j,t}}{\partial \tilde{\sigma}^2_{i,j,t}} = \frac{2(1-\theta)}{\epsilon^2} > 0$. Thus the equilibrium interest rate increases with the uncertainty about counterparty risk. Furthermore, since the first and second derivatives with respect to the threshold parameter are given by $\frac{\partial r_{i,j,t}}{\partial \epsilon} = -2(1-\theta)\frac{\sigma^2+\tilde{\sigma}^2_{i,j,t}}{\epsilon^3} < 0$ and $\frac{\partial^2 r_{i,j,t}}{\partial \epsilon^2} = 6(1-\theta)\frac{\sigma^2+\tilde{\sigma}^2_{i,j,t}}{\epsilon^4} > 0$ it follow that, ceteris paribus, the interest rate decreases for a larger threshold when default becomes a less likely event.

The partial derivative of the expected return with respect to the perception error variance is $\frac{\partial \bar{R}_{i,j,t}}{\partial \tilde{\sigma}^2_{i,j,t}} = -\frac{\partial P_{i,j,t}}{\partial \tilde{\sigma}^2_{i,j,t}} + \frac{\partial 1-P_{i,j,t}}{\partial \tilde{\sigma}^2_{i,j,t}} r_{i,j,t} + (1-P_{i,j,t})\frac{\partial r_{i,j,t}}{\partial \tilde{\sigma}^2_{i,j,t}} = -\frac{\epsilon(1+r)\theta}{(\epsilon^2+\sigma^2+\tilde{\sigma}^2_{i,j,t})^2} < 0$. These terms show the channels through which increasing uncertainty about counterparty risk affects the expected return. First, it decreases $\bar{R}_{i,j,t}$ as $\frac{\partial P_{i,j,t}}{\partial \tilde{\sigma}^2_{i,j,t}} > 0$ and hence loss given default becomes more likely. Second, it increases the risk premium that is obtained if the borrower survives. However, the net effect is negative and thus the expected return decreases for a larger perception error variance.

3.4 Peer Monitoring, Counterparty Search and Transaction Volumes

Banks can engage in costly peer monitoring targeted at mitigating asymmetric information problems about counterparty risk. Therefore, we introduce the $(N \times 1)$ vector $m_{i,t} = (m_{i,1,t}, ..., m_{i,N,t})'$ with each $m_{i,j,t} \in \mathbb{R}^+_0$ describing bank i's monitoring of bank j. In particular, $m_{i,j,t}$ denotes the expenditure that bank i incurred in period t in monitoring bank j. The *added information* that bank i acquires about bank j in period t is assumed to be a linear function of the monitoring expenditure in period t and the occurrence of transaction $l_{i,j,t}$ during the trading session t,

$$\phi_{i,j,t} = \phi(m_{i,j,t}, l_{i,j,t}) = \beta_\phi + \beta_{1,\phi} m_{i,j,t} + \beta_{2,\phi} l_{i,j,t}. \quad (3)$$

The added information affects the perception error variance in future periods, compare equation (1). By allowing $\phi_{i,j,t}$ to be a function of both $l_{i,j,t}$ and $m_{i,j,t}$, we distinguish between (costly) active information acquisition such as costly creditworthiness checks and freely obtained information and trust building via repeated interaction.

Bilateral Nash bargaining between any banks i and j in the market occurs only if these two banks have established a contact. This is an important consequence of the over-the-counter structure of interbank markets, see Ashcraft and Duffie (2007) and Afonso and Lagos (2012). Therefore, we introduce a binary variable $B_{i,j,t}$ that indicates if bank i and j are connected at time t and bargaining as described in the previous subsection is possible. Specifically, $B_{i,j,t}$ is a Bernoulli random variable with success probability $\lambda_{i,j,t}$ that can be influenced by the search efforts of bank j directed towards lender i

$$B_{i,j,t} \sim \text{Bernoulli}(\lambda_{i,j,t}) \text{ with } \lambda_{i,j,t} = \lambda(s_{j,i,t}). \quad (4)$$

The variable $s_{j,i,t} \in \mathbb{R}_0^+$ captures the search cost incurred by bank j (with a liquidity deficit) when approaching lender i. Hence, we assume loans are borrower initiated in the sense that banks with a liquidity deficit approach potential lender banks for bargaining. We collect all search efforts of bank j in the $(N \times 1)$ vector $s_{j,t} = (s_{1,i,t}, ..., s_{N,i,t})'$.

For the matching technology we assume that for increasing search efforts two banks are more likely to establish a contact and engage in interest rate negotiations. Specifically, we model the mean of the Bernoulli $B_{i,j,t}$ by a logistic function

$$\lambda_{i,j,t} = \lambda(s_{j,i,t}) = \frac{1}{1 + \exp(-\beta_\lambda(s_{j,i,t} - \alpha_\lambda))}, \quad (5)$$

with $\beta_\lambda > 0$ and $\alpha_\lambda > 0$.Hences, if $\beta_\lambda \to \infty$ this function converges to a step function that corresponds to a deterministic link formation at fixed cost α_λ. Note that for $s_{j,i,t} = 0$ we still have $\lambda_{i,j,t} > 0$, so even with zero search expenditure there is still a positive contacting probability that allows bargaining. Compare also the extended use of logistic transformations with linear index functions in the discrete choice literature, in particular the trading relationship model by Weisbuch et al. (2000).

Once a contact between two banks is established and bilateral Nash bargaining is successful, interbank lending takes place. This event is captured by the binary link variable that indicates an interbank loan of positive amount from lending bank i to borrowing bank j,

$$l_{i,j,t} = \begin{cases} 1 & \text{if } B_{i,j,t} = 1 \wedge r_{i,j,t} \leq r \\ 0 & \text{otherwise .} \end{cases} \tag{6}$$

Each granted interbank loan is characterized by a price-volume tuple $(r_{i,j,t}, y_{i,j,t})$ that represents the loan characteristics. The bilateral interest rate $r_{i,j,t}$ is the outcome of the bargaining process, see Equation 2. The granted loan amount $y_{i,j,t}$ is given by the largest feasible amount that the banks can exchange given their current liquidity shocks

$$y_{i,j,t} = \min\{\zeta^j_{i,t}, -\zeta^i_{j,t}\}\mathbb{I}(\zeta^j_{i,t} \geq 0)\mathbb{I}(\zeta^i_{j,t} \leq 0), \tag{7}$$

where the superscripts i and j indicate that liquidity shocks are counterparty specific realizations of the liquidity shocks distributed as described in subsection 3.1. Thus within each period t for each bank $2(N-1)$ liquidity shocks are realized.[11]

Because the volumes of granted loans are exogenously determined, the interest rates are for sufficiently good risk assessment directly affected by only monitoring effort of bank i and matching only by search efforts of bank j. Thus we abstract from credit rationing on the intensive margin of volumes. The model hence focuses on explaining the extensive margin and the variation in interest rates. Note also that we do not address liquidity hoarding for precautionary reasons and solely concentrate on the role of counterparty risk uncertainty.

3.5 Profit Maximization and Optimal Dynamic Monitoring and Search

Each bank $i \in \{1, ..., N\}$ faces the dynamic problem of allocating resources to monitoring counterparties and choosing which bank to approach for transaction to maximize expected discounted payoffs of interbank trading. Formally the infinite-horizon dynamic optimization problem of each bank is given by

$$\max_{\{m_{i,t}, s_{i,t}\}} \mathbb{E}_t \sum_{s=t}^{\infty} \left(\frac{1}{1+r^d}\right)^{s-t} \pi_{i,s}(m_{i,s}, s_{i,s}), \tag{8}$$

[11] In a previous version of the paper we assumed similarly to Babus (2013) and Vuillemey and Breton (2014) that at each time instance each bank is paired with at most one counterparty (for example paring two banks randomly at each time instance) to avoid solving a complicated multilateral bargaining problem at each time. For a given observed data frequency (in our analysis daily) simulated data is then aggregated to allow for nodes with multiple links.

where $\pi_{i,t}$ denotes the interbank profit of bank i at time t, r^d denotes the discount rate, and the maximization is subject to the restrictions imposed by the structure laid down in Sections 3.1-3.4.

The only unspecified function in the objective function above is the profit function $\pi_{i,s}(m_{i,s}, s_{i,s})$. Naturally, period t expected interbank profits of bank i written in terms of surplus over the outside options are given by

$$\pi_{i,t} = \sum_{j=1}^{N} l_{i,j,t}\bar{R}_{i,j,t}y_{i,j,t} + l_{j,i,t}(r - r_{j,i,t})y_{j,i,t} - m_{i,j,t} - s_{i,j,t}.$$

Note that the intertemporal problem is made operational by conditioning on the equilibrium interest rates $r_{i,j,t}$ characterized in section 3.3. Hence, in this section these interest rates appear as a restriction on the optimization instead of an argument of the objective function.

Unfortunately, it is computationally infeasible to work with the exact solution to the optimization problem for two reasons. First, attempting to use N different policy functions for the N different banks would make simulation and estimation prohibitively time-consuming even in large computer clusters. We therefore impose that all banks make use of a 'general' policy function that is derived from the optimization of banks with liquidity shock distributions fixed at $\mathcal{N}(\mathbb{E}(\mu_{\zeta_i}), \mathbb{E}(\sigma^2_{\zeta_i}))$. This allows us to derive a unique policy function that can be used by all banks to map state variables into decision variables. Second, the lack of smoothness of the dynamic optimization problem prevents us from obtaining analytic optimality conditions. We consider therefore an approximate smooth problem where we replace the step functions by a continuously differentiable function.[12] This allows us to use the calculus of variations that is well understood and the most widely applied method to solve constrained dynamic stochastic optimization problems in structural economics; see e.g. Judd (1998) and DeJong and Dave (2006). We thus obtain Euler equations that constitute approximate solutions to the original non-differentiable model.

Substituting out all definitions except for the law of motion for $\tilde{\sigma}^2_{i,j,t}$, we can write the Lagrange function with multiplier $\mu_{i,j,t}$ given by

$$\mathcal{L} = \mathbb{E}_t \sum_{s=t}^{\infty} \left(\frac{1}{1+r^d}\right)^{s-t} \sum_{j=1}^{N} \pi_{i,j,t}(m_{i,j,t}, s_{i,j,t}, \tilde{\sigma}^2_{i,j,t}) + \mu_{i,j,t}(\xi(m_{i,j,t}, \tilde{\sigma}^2_{i,j,t}) - \tilde{\sigma}^2_{i,j,t+1}),$$

where we made the arguments that can be influenced by bank i's decision explicit. The Euler

[12]Specifically, we use a logistic functions $l(x) = \frac{1}{1+\exp(-\beta_x x)}$ with large scale parameter β_x to approximate the step function $\mathbb{I}(x \geq 0)$. In the original problem, the step function is entering in equation (6) as $l_{i,j,t} = \eta_{i,j,t} \cdot \mathbb{I}(r_{i,j,t} \leq r)$. Note that for a growing scale parameter the logistic transformation approximates the step function arbitrary well.

equations that establish the first-order-conditions to the infinite-horizon nonlinear dynamic stochastic optimization problem can then be obtained by optimizing the Lagrange function w.r.t. to the control variables and the dynamic constraints, see e.g. Heer and Maußner (2005).

Under usual regularity conditions the integration and differentiation steps can be interchanged and we obtain

$$\begin{aligned}
\frac{\partial \mathcal{L}}{\partial m_{i,j,t}} &= 0 \;\Leftrightarrow\; \mathbb{E}_t\Big[\frac{\partial \pi_{i,j,t}}{\partial m_{i,j,t}} + \mu_{i,j,t}\frac{\partial \xi_{i,j,t}}{\partial m_{i,j,t}}\Big] = 0 \\
\frac{\partial \mathcal{L}}{\partial \tilde{\sigma}^2_{i,j,t+1}} &= 0 \;\Leftrightarrow\; \mathbb{E}_t\Big[-\mu_{i,j,t} + \frac{1}{1+r^d}\left(\frac{\partial \pi_{i,j,t+1}}{\partial \tilde{\sigma}^2_{i,j,t+1}} + \mu_{i,j,t+1}\frac{\partial \xi_{i,j,t+1}}{\partial \tilde{\sigma}^2_{i,j,t+1}}\right)\Big] = 0 \\
\frac{\partial \mathcal{L}}{\partial s_{i,j,t}} &= 0 \;\Leftrightarrow\; \mathbb{E}_t\Big[\frac{\partial \pi_{i,j,t}}{\partial s_{i,j,t}} + \frac{1}{1+r^d}\frac{\partial \pi_{i,j,t+1}}{\partial s_{i,j,t}}\Big] = 0 \\
\frac{\partial \mathcal{L}}{\partial \mu_{i,j,t}} &= 0 \;\Leftrightarrow\; \mathbb{E}_t\Big[\tilde{\sigma}^2_{i,j,t+1} - \xi(\phi_{i,j,t}, \tilde{\sigma}^2_{i,j,t})\Big] = 0
\end{aligned}$$

for all counterparties $j \neq i$ and all t. Substituting out the Lagrange multipliers and taking fixed values at time t out of the expectation gives the Euler equation for the optimal monitoring path,

$$\frac{\partial \pi_{i,j,t}}{\partial m_{i,j,t}} = \frac{1}{1+r^d}\frac{\partial \xi_{i,j,t}}{\partial m_{i,j,t}}\mathbb{E}_t\left(\frac{\partial \xi_{i,j,t+1}}{\partial \tilde{\sigma}^2_{i,j,t+1}}\frac{\frac{\partial \pi_{i,j,t+1}}{\partial m_{i,j,t+1}}}{\frac{\partial \xi_{i,j,t+1}}{\partial m_{i,j,t+1}}} - \frac{\partial \pi_{i,j,t+1}}{\partial \tilde{\sigma}^2_{i,j,t+1}}\right). \tag{9}$$

that equates marginal cost and discounted expected future marginal benefits of monitoring. Unlike monitoring expenditures, search becomes effective in the same period it is exerted and does not directly alter future matching probabilities via a dynamic constraint. Thus the first-order condition for the optimal search path is given by

$$\frac{\partial \pi_{i,j,t}}{\partial s_{i,j,t}} = -\mathbb{E}_t\frac{\partial \pi_{i,j,t}}{\partial s_{i,j,t}}, \tag{10}$$

leading to the usual marginal cost equals expected marginal benefits in each period without any discounting. Note that because the first-order conditions hold for all $j \neq i$ and the marginal cost of monitoring and search is the same across all j, the conditions also imply that (discounted) expected marginal profits of monitoring and search must be the same across different banks j.

The transversality condition for the dynamic problem is obtained as the limit to the endpoint condition from the corresponding finite horizon problem and requires that

$$\lim_{T\to\infty}\mathbb{E}_t\left[\left(\frac{1}{1+r^d}\right)^{T-2}\frac{\partial \pi_{i,j,T-1}}{\partial m_{i,j,T-1}} - \left(\frac{1}{1+r^d}\right)^{T-1}\frac{\partial \pi_{i,j,T}}{\partial \tilde{\sigma}^2_{i,j,T}}\frac{\partial \xi_{i,j,T-1}}{\partial m_{i,j,T-1}}\right] = 0.$$

Thus in the limit the expected marginal cost of investing in monitoring must be equal to the expected marginal return.

3.6 Simulating from Optimal Policy Functions Under Adaptive Expectations

Following the bulk of the literature on stochastic dynamic modeling, see e.g. DeJong and Dave (2006) and Ruge-Murcia (2007), we simulate from the structural model by first deriving the optimal policy rules, linearizing them and then adopting an expectation generating mechanism that delivers the reduced form of the model.

3.6.1 Solution to FOCs

The Euler equations for the optimal monitoring decisions given in equation (9) can be written as

$$\mathbb{E}_t f(m_{i,j,t}, \tilde{\sigma}^2_{i,j,t}, \tilde{\sigma}^2_{i,j,t+1}, \lambda_{i,j,t+1}, y_{i,j,t+1}) = 0.$$

Note that due to the specific functional form of $\xi_{i,j,t}$ the first order conditions do not depend on $m_{i,j,t+1}$. As discussed above, we derive a common policy rule based on expected loan volumes under the central liquidity shock distribution with mean parameter $\mathbb{E}(\mu_{\zeta_i}) = \mu_\mu$ and variance parameter $\mathbb{E}(\sigma^2_{\zeta_i}) = \exp(\mu_\sigma + \sigma^2_\sigma/2)$.

Therefore, we linearize the function f by a first-order Taylor expansion around a point where the network is stable in some sense. We therefore introduce the concept of the *mean steady state* denoted by $(\tilde{m}_{i,j}, \tilde{\tilde{\sigma}}^2_{i,j}, \tilde{\tilde{\sigma}}^2_{i,j}, \tilde{\lambda}_{i,j}, \tilde{y}_{i,j})$. The mean steady-state does not correspond to the steady-state of the system where all shocks are set to zero ($\zeta_{i,t} = 0 \ \forall i, t$), but it is obtained from setting $y_{i,j,t}$ at its expectation $\tilde{y}_{i,j} := \mathbb{E}_g(y_{i,j,t})$, where $\mathbb{E}_g$ denotes the expectations under the central liquidity shock distribution, and then solving for the time-invariant triple $(\tilde{m}_{i,j}, \tilde{\lambda}_{i,j}, \tilde{\tilde{\sigma}}^2_{i,j})$ such that the Euler equations hold.[13]

In the following expansion we write $h_x := \frac{\partial h(x,y)}{\partial x}$ and use $\hat{x} := x - \tilde{x}$ to denote deviation from mean steady-state values. Applying the first-order Taylor expansion around the mean steady-state gives

$$f \approx \tilde{f} + f_{m_{i,j,t}} \hat{m}_{i,j,t} + f_{\tilde{\sigma}^2_{i,j,t}} \hat{\tilde{\sigma}}^2_{i,j,t} + f_{\tilde{\sigma}^2_{i,j,t+1}} \hat{\tilde{\sigma}}^2_{i,j,t+1} + f_{\lambda_{i,j,t+1}} \hat{\lambda}_{i,j,t+1} + f_{y_{i,j,t+1}} \hat{y}_{i,j,t+1}$$

[13] We do not expand the function f around the usual steady-state because at this point $\hat{y}_{i,j} = 0$ for $\mu_\mu = 0$, such that it constitutes a critical point where all partial derivatives are zero.

where $\tilde{f} := f(\tilde{m}_{i,j}, \tilde{\tilde{\sigma}}^2_{i,j}, \tilde{\tilde{\sigma}}^2_{i,j}, \tilde{\lambda}_{i,j}, \tilde{y}_{i,j})$ and all derivatives are evaluated at the expansion point, i.e. the mean steady-state. Note that $\tilde{f} = 0$ by construction.

We then obtain the approximate Euler equation for monitoring as

$$\mathbb{E}_t\Big[f_{m_{i,j,t}}\hat{m}_{i,j,t} + f_{\sigma^2_{i,j,t}}\hat{\tilde{\sigma}}^2_{i,j,t} + f_{\tilde{\sigma}^2_{i,j,t+1}}\hat{\tilde{\sigma}}^2_{i,j,t+1} + f_{\lambda_{i,j,t+1}}\hat{\lambda}_{i,j,t+1} + f_{y_{i,j,t+1}}\hat{y}_{i,j,t+1}\Big] = 0$$

which we rearrange to get the linear policy function

$$m_{i,j,t} = a_m + b_m\tilde{\sigma}^2_{i,j,t} + c_m\mathbb{E}_t\tilde{\sigma}_{i,j,t+1} + d_m\mathbb{E}_t\lambda_{i,j,t+1} + e_m\mathbb{E}_t y_{i,j,t+1}. \tag{11}$$

This equation shows that the optimal monitoring expenditures of bank i towards bank j depends on the current state of uncertainty, the expected future uncertainty, the expected volume of the loan and on the expected probability of being contacted by bank j.

Because the derivative of the probability of success of the Bernoulli variable, $\lambda'(s_{i,j,t})$, is invertible, we obtain an analytical solution to the first order-condition in equation that characterizes any interior solution with positive search levels and obtain

$$s(\Delta_{i,j,t}) := 1/\beta_\lambda \log\Big(0.5(\sqrt{\Delta_{i,j,t}\beta_\lambda(\Delta_{i,j,t}\beta_\lambda - 4)} + \Delta_{i,j,t}\beta_\lambda - 2)e^{\alpha_\lambda\beta_\lambda})\Big) \tag{12}$$

for $\Delta_{i,j,t}\beta_\lambda(\Delta_{i,j,t}\beta_\lambda - 4) \geq 0$ where $\Delta_{i,j,t} := \mathbb{E}_t[y_{j,i,t}(r - r_{j,i,t})]$ is the expected surplus (relative to the outside option r) of bank i when borrowing funds from lender j. The optimal search level of bank i towards bank j at time t is thus given by

$$s_{i,j,t} = \begin{cases} s(\Delta_{i,j,t}) & \text{for } \; \Delta_{i,j,t}\lambda(s(\Delta_{i,j,t})) - s(\Delta_{i,j,t}) \geq 0 \\ 0 & \text{for } \; \Delta_{i,j,t}\lambda(s(\Delta_{i,j,t})) - s(\Delta_{i,j,t}) < 0. \end{cases} \tag{13}$$

That is for positive expected return net of search cost the solutions satisfies Equation (12). Note that the optimal $s_{i,j,t}$ is a non-linear function of the expected surplus $\Delta_{i,j,t}$ with $s(\cdot)' > 0$. Note that $\lambda(0) > 0$ and hence even without search efforts two banks will eventually get connected to each other and bargain about loan outcomes.

3.6.2 Adaptive Expectations

The optimal monitoring and search levels depend on expectations about bilateral credit availability and conditions. We assume that banks form bank-specific *adaptive expectations* about future credit conditions in the market. However, banks are not only uncertain about future variables but also about present and past credit conditions at other banks. Therefore, the decisions of banks are the result of a complex web of expectations about past, present and future trading conditions that change every period as banks search, monitor and ultimately have contact with each other. This is an essential feature of the opaque interbank market structure, where information is not revealed in a central manner, but banks learn about credit condition at other banks only through contact and engaging in trade.

In particular, the adaptive expectation formation of bank i concerning variable $x_{i,j,t}$ draws from past experience according to an exponentially weighted moving average (EWMA)

$$\mathbb{E}_t x_{i,j,t+1} := x^*_{i,j,t} = (1-\lambda_x)x^*_{i,j,t-1} + \lambda_x x_{i,j,t}, \tag{14}$$

where all variables are in deviation from the mean steady-state values. In particular we use this forecasting rule for variables that are always observed by bank i (for instance, $\hat{m}_{i,j,t}$, the own monitoring effort). Due to the over-the-counter structure a bank however learns about credit condition at *other* banks only once upon contact. We incorporate this crucial feature of decentralized interbank markets by assuming that bank i uses the following forecasting rule,

$$x^*_{i,j,t} = (1-\lambda_x)x^*_{i,j,t-1} + \lambda_x B_{i,j,t} x_{i,j,t}. \tag{15}$$

Recall that $B_{i,j,t}(s_{j,i,t-1}) = 1$ denotes an 'open' connection. Hence new information about a counterparty is added to the last forecast only if the banks where in contact, otherwise the last forecast is not maintained but discounted by a factor $(1-\lambda_x)$. Thus if bank i and j are not in contact for a long time their expectations converge to the mean steady-state values. In both cases the initial value is assumed to be given by $x^*_0 = x_0$ and the parameter $\lambda_x \in (0,1)$ determines the weight of the new observations at t.

The formulation of the expectation mechanism completes the model description. From the structural model a reduced form representation can be obtained that allows simulating from the parametric model under some fix parameter vector, details on the reduced form representation and stability conditions are provided in Appendix B.

4 Parameter Estimation

We now turn to the estimation of the structural model parameters using loan level data from the Dutch overnight interbank lending market. Due to the complexity of the model (non-linearity and non-standard distributions) the likelihood function is not known even up to a constant, rendering maximum likelihood estimation or Bayesian methods impossible. We therefore resort to the simulation-based method of indirect inference that is building on an appropriate set of auxiliary statistics to estimate the structural model parameters.

4.1 Auxiliary Statistics and Indirect Inference

Following the principle of indirect inference introduced in Gourieroux et al. (1993), we estimate the vector of parameters $\boldsymbol{\theta}_T$ by minimizing the distance between the auxiliary statistics $\hat{\boldsymbol{\beta}}_T$ obtained from the observed data $X_1, ..., X_T$, and the average of the auxiliary statistics $\tilde{\boldsymbol{\beta}}_{TS}(\theta) := (1/S)\sum_{s=1}^{S} \tilde{\boldsymbol{\beta}}_{T,s}(\theta)$ obtained from S simulated data sets $\{\tilde{X}_{1,s}(\boldsymbol{\theta}), ..., \tilde{X}_{T,s}(\boldsymbol{\theta})\}_{s=1}^{S}$ generated under $\theta \in \Theta$. Formally the indirect inference estimator is thus given as

$$\hat{\boldsymbol{\theta}}_T := \underset{\boldsymbol{\theta} \in \Theta}{\text{argmax}} \left\| \hat{\boldsymbol{\beta}}_T - \frac{1}{S} \sum_{s=1}^{S} \tilde{\boldsymbol{\beta}}_{T,s}(\boldsymbol{\theta}) \right\|,$$

where Θ denotes the parameter space of $\boldsymbol{\theta}$. Under appropriate regularity conditions this estimator is consistent and asymptotically normal. In particular, consistency holds as long as, for given $S \in \mathbb{N}$, the auxiliary statistics converge in probability to singleton limits $\hat{\boldsymbol{\beta}}_T \xrightarrow{p} \boldsymbol{\beta}(\boldsymbol{\theta}_0)$ and $\tilde{\boldsymbol{\beta}}_{T,s} \xrightarrow{p} \boldsymbol{\beta}(\boldsymbol{\theta})$ as $T \to \infty$ and the so-called *binding function* $\boldsymbol{\beta} : \Theta \to \mathcal{B}$ is injective. Convergence in probability is precisely ensured through the application of a law of large numbers for strictly stationary and ergodic data, see e.g. White (2001). Similarly, asymptotic normality of the estimator is obtained if the auxiliary statistics $\hat{\boldsymbol{\beta}}_T$ and $\tilde{\boldsymbol{\beta}}_{T,s}$ are asymptotically normal, see Gourieroux et al. (1993) for details. By application of a central limit theorem, see e.g. White (2001), the asymptotic normality of the auxiliary statistics can again be obtained by appealing to the strict stationarity and ergodicity of both observed and simulated data.

The injective nature of the binding function is the fundamental identification condition which ensures that the structural parameters are appropriately described by the auxiliary statistics. This condition cannot be verified algebraically since the binding function is analytically intractable. However, identification will be ensured as long as the set of auxiliary statistics adequately describes both observed and simulated data. We hence select auxiliary statistics that provide a rich characterization of the interbank market represented by the network of bilateral loans and associated volumes and interest rates. Specifically, we explore the auto-covariance structure, higher-order moments, and a number of network statistics as auxiliary statistics. The use of means, variances and auto-covariances is in line with the bulk of the literature concerned with the estimation of structural models such as Dynamic Stochastic General Equilibrium models, see e.g. DeJong and Dave (2006) and Ruge-Murcia (2007). The use of higher-order moments such as measures of skewness and kurtosis is justified by the nonlinearity of the model and the fact that some structural parameters might be well identified by such statistics.

In addition to these standard auxiliary statistics, we base the indirect inference estimator of the network model on auxiliary statistics that characterize specifically the topological structure of the interbank lending network. In particular, our model focuses on explaining relationship lending and the sparse core-periphery structure and we hence include statistics that measures these characteristics. Thereby, we follow the large empirical literature on the structure of interbank lending networks and use few key network statistics, see e.g. Bech and Atalay (2010). Moreover, we refrain from using computationally more expensive network statistics due to the large number of simulated networks in the estimation procedure.

First, we consider global network statistic. In particular, the *density* defined as the ratio of the actual to the potential number of links is a standard measures of the connectivity of a network. A low density characterizes a sparse network with few links. The *reciprocity* measures the fraction of reciprocal links in a directed network. For the interbank market this relates to the degree of mutual lending between banks. The *stability* of a sequence of networks refers to the fraction of links that do not change between two adjacent periods. Note that all three statistics are bounded between zero and one.

Second, we include bank (node) level network statistics. The (unweighted) *in-degree* of a bank is defined as the number of lenders it is borrowing funds from, the (unweighted) *out-degree* as the number of borrowers is is lending funds to. We summarize this bank level information using the mean and standard deviation of the (in-/out-) degree distribution as well as its skewness. The (local) *clustering coefficient* of a node quantifies how close its neighbors are to being a clique (complete graph). In the interbank network it measure how many of a bank's counterparties have mutual credit exposures to each other. We compute the clustering coefficients for directed networks as proposed by Fagiolo (2007) and consider the average clustering as auxiliary statistic.

Third, we focus on simple bilateral network statistics that measure the intensity of a bilateral trading relationship based on a rolling window. Similar to Furfine (1999) and Cocco et al. (2009), we compute the number of loans given from bank i to bank j during the last week and denote this variable by $l^{rw}_{i,j,t}$. We then compute a cross-sectional correlation between these relationship variables and loan outcomes at time t (decision to grant a loan and interest rate).

We compute all described network statistics for the each lending network within the sequence of networks such that we obtain a sequence of network statistics associated with the sequence of networks. We then obtain the unconditional means, variance and/or auto-correlation of these sequences as auxiliary statistics and base the parameter estimations on the values of the auxiliary statistics only. In Appendix C we provide the formulae of the described network statistics. For further details on network statistics in economics see Jackson (2008).

4.2 Data Description

The original raw data used in the estimation procedure comprises the bilateral lending volumes and interest-rates practiced on a daily basis in the over-night lending market between Dutch banks. In particular, we make use of a confidential transaction level dataset of interbank loans that has been compiled by central bank authorities based on payment records in the European large value payment system TARGET2. The panel of interbank loans has been inferred using a modified and improved version of the algorithm proposed by Furfine (1999). This algorithm matches payment legs between pairs of banks and classifies those as interbank loans depending on the size of the initial payment and size and date of candidate repayments, for details on the data set and methodology see Heijmans et al. (2011) and Arciero et al. (2013)

Compared to interbank lending data derived from the US fedwire data and payment systems of other countries, our dataset has three major advantages that are crucial for the high data quality. First, TARGET2 payments have a flag for interbank credit payments restricting the universe of all payments to be searched by the algorithm. Second, information on the actual sender and receiver bank is available. Unlike settlement banks, sender and receiver bank are the ultimate economic agents involved in the contract, in particular the sender bank is exposed to inherent counterparty credit risk that is at the core of our model. Third, and most importantly, euro area interbank lending data derived from Furfine-type algorithms has been cross-validated with official Spanish and Italian interbank transaction level data yielding type I errors of less than 1%, i.e. less than 1% of all payments are incorrectly paired and classified as interbank loans, see Arciero et al. (2013) and de Frutos et al. (2014).

In the estimation we use data of daily frequency for the period between 1 February 2008 until 20 March 2011 ($T = 810$ trading days), including the Lehman failure on 15 September 2008. Because our model does not address lending in different maturities we resort to the most active overnight segment. Moreover, for computational reasons we focus on interbank lending between the $N = 50$ largest banks according to their trading frequency (as both borrower and lender) throughout the entire sample. As a result, the observed data from which the auxiliary statistics are obtained consists in essence of three $N \times N \times T$ arrays with elements $l_{i,j,t}$, $y_{i,j,t}$ and $r_{i,j,t}$ observed at daily frequency.[14] The arrays for $y_{i,j,t}$ and $r_{i,j,t}$ contain missing values if and only if $l_{i,j,t} = 0$.

Table 1: Descriptive statistics. The table reports moment statistics for different sequences of network statistics and cross-sectional correlations that characterize the sequence of observed Dutch unsecured interbank lending networks. The statistics are computed on a sample of daily frequency from 1 February 2008 to 30 April 2011.

Statistic	Mean	Std	Autocorr
Density	0.0212	0.0068	0.8174
Reciprocity	0.0819	0.0495	0.2573
Stability	0.9818	0.0065	0.8309
Mean out-/indegree	1.0380	0.3323	0.8174
Mean clustering	0.0308	0.0225	0.4149
Corr$(r_{i,j,t}, l^{rw}_{i,j,t-1})$	-0.0716	0.1573	0.4066
Corr$(l_{i,j,t}, l^{rw}_{i,j,t-1})$	0.6439	0.0755	0.4287
Mean log-volume	4.1173	0.2818	0.4926
Mean rate	0.2860	0.3741	0.9655

Table 1 shows key summary statistics of the data used in the analysis, more detailed summary statistics are provided in Appendix D. Note that: (i) the moments of traded volumes are for values stated in (logarithm of) millions of euros; (ii) the moments of interest rates are reported in percentage points per annum above the ECB deposit facility rate (lower bound of the interest rate corridor); (iii) the daily interbank network is very sparse with mean density 0.02 (on average 1.04 lenders and borrowers) and low clustering; (iv) the distribution of interest rates, volumes, degree centrality and clustering are highly skewed, see the appendix. It is also important to highlight here that the high auto-correlation of the density, the high stability of the network as well as the positive expected correlation between current period lending and past lending activity can be seen as evidence of the construction of 'trust relations' between banks and shows that past trades affect future trading opportunities. Similarly, the negative expected correlation between past lending activity and present interest rates provide evidence of reduction in perceived risk that may be justified by monitoring efforts as postulated by the proposed structural model.

Figure 2 graphs the time evolution of the daily network density, stability, average (log) volume, total volume, and mean and standard deviation of the daily spreads throughout the sample. From the plots we see that the network density and total trading volume (in millions of euros) declined after Lehman's failure on 15 September 2008 which is indicated by the

[14]The dataset contains only loan of at least 1 million euros volume as typically banks with shocks below that value do not go to the market. Therefore, Equation (7) for the volumes of granted loans changes accordingly.

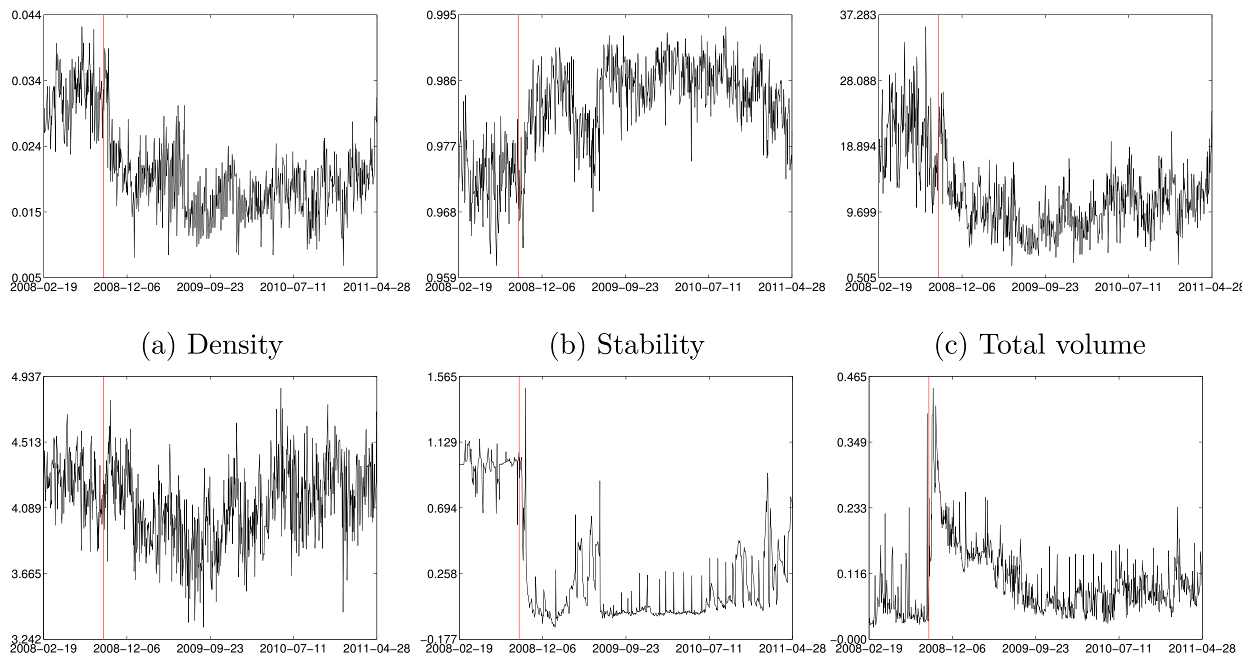

(a) Density (b) Stability (c) Total volume

(d) Mean (log) volume (e) Mean spread (f) Stdev spread

Figure 2: Time series plots of daily network density, stability, total traded volume, and mean (log) volume, mean spread, and standard deviation of granted loans from February 2008 to April 2011. Vertical red line corresponds to Lehman's failure on 15 September 2008.

vertical red line. At the same time the network stability and the cross-sectional standard deviation of interest rate spreads increase. Moreover, the mean spreads of granted loans are close to the deposit facility as of October 2008. Further, the plots reveal that the data exhibits well documented end-of-maintenance effects that we clean out in the construction of the auxiliary statistics by regressing each sequence of network statistics on end-of-maintenance period dummies before computing auxiliary statistics.

4.3 Estimation Results

We next turn to the estimation results of the interbank network model. Table 2 shows the point estimates, standard errors and 90% confidence intervals of the structural parameters using a quadratic objective function and $S = 24$ simulated network paths each of length $T^* = 3000$ with 1000 periods burned to minimize dependence on initial values. The inference is based on the auxiliary statistics $\hat{\boldsymbol{\beta}}_T$ that are reported in Table 4. Appendix E contains details on the choice of the objective function. Note that some of the structural parameters are calibrated as these are not identified by the data. For example, it is clear that several combinations of β_σ, $\beta_{1,\phi}$ and $\beta_{2,\phi}$ imply the same distribution for the data, and hence, also for the auxiliary statistics. The same applies for ϵ and σ. Further, we fix the common default threshold ϵ and the common true variance of the financial distress σ^2 to obtain a upper bound on the true probability of default of 0.01. Naturally, standard errors and confidence intervals are not provided for calibrated parameters. An alternative, calibrated parameter vector ($\boldsymbol{\theta_a}$) which equals $\hat{\boldsymbol{\beta}}_T$ but restricts the effects of monitoring to zero is presented for comparison with the indirect inference estimates.

Table 2: Estimated parameter values. The table reports the estimated structural parameters ($\hat{\boldsymbol{\theta}}_T$) and corresponding standard errors and 90% confidence bounds. For calibrated parameters no standard errors and confidence bounds are reported. The indirect inference estimator is based on $S = 24$ simulated network sequences of length $T^* = 3000$. The parameter $\boldsymbol{\theta}_a$ represents an alternative, calibrated model parametrization. Note also that $\sigma^*_\mu = \log(\sigma_\mu)$.

Structural parameters		Calibrated $\boldsymbol{\theta}_a$	Estimated $\hat{\boldsymbol{\theta}}_T$	St.Errors ste($\hat{\boldsymbol{\theta}}_T$)	90% Bounds LB	UB
Added information	α_ϕ	-1.5000	-1.5000	-	-	-
	$\beta_{\phi,1}$	0.0000	9.6631	0.0006	9.6619	9.6643
	$\beta_{\phi,2}$	0.0001	0.0001	0.0445	-0.0871	0.0873
Perception error	α_σ	1.2890	1.2890	0.0028	1.2835	1.2945
	β_σ	2.0000	2.0000	-	-	-
	γ_σ	0.6648	0.6648	0.0183	0.6289	0.7007
	δ_σ	0.3383	0.3383	0.0451	0.2499	0.4267
Search technology	α_λ	0.0001	0.0001	0.1159	-0.2271	0.2273
	β_λ	72.8331	72.8331	0.0006	72.8319	72.8343
Liquidity shocks	μ_μ	0.0000	0.0000	-	-	-
	σ^*_μ	1.9903	1.9903	0.0228	1.9456	2.0350
	μ_σ	1.9492	1.9492	0.0218	1.9065	1.9919
	σ_σ	1.9810	1.9810	0.0213	1.9393	2.0227
	ρ_ζ	-0.7826	-0.7826	0.0423	-0.6997	-0.8655
Expectations	λ^l	0.9278	0.9278	0.0470	0.8357	1.0199
	λ^z	0.8472	0.8472	0.0443	0.7604	0.9340
	λ^r	0.4008	0.4008	0.0466	0.3095	0.4921
	λ^σ	0.0318	0.0318	0.0414	-0.0493	0.1129
Bargaining lender	θ	0.6897	0.6896	0.0441	0.6032	0.7760
CB corridor width	r	1.5000	1.5000	-	-	-
Default threshold	ϵ	3.0000	3.0000	-	-	-
Financial distress	σ	0.1000	0.1000	-	-	-
Discount rate	r^d	0.0000	0.0000	-	-	-
Scale logistic	β_I	200.00	200.00	-	-	-

The parameter estimates reported in Table 2 are interesting in several respects. First, the estimated coefficient $\beta_{\phi,1}$ that determines the effect of peer monitoring on the added information is positive and statistically significant. Hence, we find monitoring to be a significant factor in the reduction of counterparty risk uncertainty. On the other hand, the estimated coefficient that determines the effect of the occurrence of a trade is very low and statistically insignificant. Moreover, the autoregressive parameter γ_σ is estimated to be 0.66 and indicating some autocorrelation in bilateral credit risk uncertainty in the absence of new information. Further, note the relatively large intercept of the autoregressive log-variance process and scaling of the shocks to the perception error variance, δ_σ.

Second, the positive estimate for α_λ and β_λ shows that counterparty search is a crucial feature in the formation of interbank networks. In particular, the positive estimate for β_λ suggests that links are not formed at random but are strongly influenced by banks' search towards preferred counterparties. It also highlights the effect of expected profitability and counterparty selection. In this respect, the positive point estimate for the expectation parameter of available interest rates, λ^r, and available loan volumes, λ^z, indicate persistent expectations about credit conditions. Similarly, the values of λ^l indicate a strong persistence in the expectations of being contacted by a specific borrower. These persistent expectation eventually contribute to the high persistence of bilateral trading relationship and the entire interbank network.

Third, the estimated values of the central liquidity distribution that parameterizes banks' liquidity shock distributions point towards considerably heterogeneity in liquidity shocks. The estimated log normal distribution implies that there are few banks with very large liquidity shock variances that are very active players in the market. Moreover the notion that some banks are structural liquidity providers or supplier is supported by the positive estimate of the variance parameter of the mean. Note also the estimated negative correlation parameter indicating that banks with a small liquidity shock variance typically have a positive mean.

Table 3: Coefficients of linear policy rule for optimal monitoring

Variable	$\tilde{\sigma}_{i,j,t}$	$\mathbb{E}_t\tilde{\sigma}_{i,j,t+1}$	$\mathbb{E}_t\lambda_{i,j,t+1}$	$\mathbb{E}_t y_{i,j,t+1}$
Coefficient	0.0024	-0.0043	0.0348	0.0019

In Table 3 we report the coefficients of the linear policy rule for the optimal monitoring levels as implied by the estimated parameters, expressed in deviations from their mean steady-state values. It is particular noteworthy that the optimal monitoring level towards a particular bank depends positively on the expected probability of being approached by this bank to borrow funds during future trading sessions, $\mathbb{E}_t\lambda_{i,j,t+1}$. Indeed this positive coefficient and the significantly positive effect of search on link formation creates the interrelation between monitoring and search as the source of persistent interbank relationship lending.

Moreover, note that the current state of uncertainty positively affects monitoring during this period, higher expected future uncertainty however reduces these efforts. The positive coefficient of the amount of granted loans shows that banks prefer to monitor those counterparties where they expect to trade larger volumes as the surplus that can be generated by reducing credit risk uncertainty is larger. This implies that banks with on average opposite liquidity shocks will monitor each other more closely as they will on average exchange funds of larger quantity.

We next analyze the model fit and auxiliary statistics. Table 4 shows how the estimated structural parameter vector $\hat{\boldsymbol{\theta}}_T$ produces an accurate description of the data when compared to the alternative calibrated parameter vector $\boldsymbol{\theta}_a$ stated in Table 2 where the effects of monitoring on the perception error variance are restricted to be zero.

First note the remarkable improvement in model fit compared to the calibrated example, brought about by the indirect inference estimation, as judged by (i) the value of the (log) criterion function that is about 54 times smaller for the estimated model, and (ii) the comparison between auxiliary statistics obtained from observed data, data simulated at the calibrated parameter, and data simulated at the estimated parameters. For instance, the Euclidean norm and the sup norm of the difference between observed and simulated auxiliary statistics are about 3.5 and 5 times larger under the calibration without monitoring, respectively.

A closer look at individual auxiliary statistics reveals several interesting features of the estimated model. First, it is important to highlight the significant improvement in the fit of the density compared to the calibrated example. In fact, the estimated model matches the sparsity of the Dutch interbank network very well with a density of about 0.02. Likewise, the present structural model provides a very accurate description of the high stability of the network with values of 0.98. Similarly, the average clustering coefficient improves considerably compared to the calibrated model and matches the data very well with a small value of 0.03. Moreover, the estimated model implies that about 6.3% of all links are of reciprocal nature, compared to 8.2% in the observed data. A comparison of observed and simulated auxiliary statistics shows that the model is also able to replicate well the first three moments of the observed degree distribution.[15] In particular, the estimated model generates a high positive skewness of both the in-degree and out-degree distribution, compare the simulated skewness of 2.4 and 2.3 with the observed one 2.8 and 2.4, respectively. Similarly, the standard deviation of both degree distributions are quite accurate with values of 1.7 and 1.7 as compared to

[15]Note that the density is just a rescaled version of the average degree centrality, we did not include the density in the estimation but show it for convenience in Table 4.

Table 4: Auxiliary network statistics. The table reports the values of the observed auxiliary statistics $\hat{\boldsymbol{\beta}}_T$ used in the indirect inference estimation along with the HAC robust standard errors. The simulated average of the auxiliary statistics $\tilde{\boldsymbol{\beta}}_{TS}$ is shown for the estimated parameter vector $\hat{\boldsymbol{\theta}}_T$ and the alternative calibration $\boldsymbol{\theta}_a$. The observed statistics are computed on a sample of daily frequency from 1 February 2008 to 30 April 2011 of size $T = 810$. Objective function is quadratic form, see appendix for details.

	Simulated		Observed	
	Calibrated	Estimated		
Auxiliary statistic	$\tilde{\boldsymbol{\beta}}_{TS}(\boldsymbol{\theta}_a)$	$\tilde{\boldsymbol{\beta}}_{TS}(\hat{\boldsymbol{\theta}}_T)$	$\hat{\boldsymbol{\beta}}_T$	ste($\hat{\boldsymbol{\beta}}_T$)
Density (mean)[a]	0.1121	0.0193	0.0212	0.0026
Reciprocity (mean)	0.0453	0.0627	0.0819	0.0029
Stability (mean)	0.8247	0.9795	0.9818	0.0025
Avg clustering (mean)	0.1097	0.0347	0.0308	0.0027
Avg degree (mean)	5.4948	0.9441	1.0380	0.1291
Std outdegree (mean)	3.2901	1.6547	1.8406	0.0918
Skew outdegree (mean)	0.4512	2.3649	2.8821	0.3537
Std indegree (mean)	4.7450	1.6950	1.6001	0.0995
Skew indegree (mean)	0.3300	2.2801	2.4030	0.3143
Corr($r_{i,j,t}, l^{rw}_{i,j,t-1}$) (mean)	0.0000	-0.1231	-0.0716	0.0113
Corr($l_{i,j,t}, l^{rw}_{i,j,t-1}$) (mean)	0.2345	0.6001	0.6439	0.0107
Avg log volume (mean)	2.8298	3.9422	4.1173	0.0516
Std log volume (mean)	1.0547	1.0865	1.6896	0.0200
Skew log volume (mean)	-0.1187	-0.1357	-0.3563	0.0317
Avg interest rates (mean)	1.0348	1.1353	0.2860	0.1331
Std interest rates (mean)	0.0000	0.1004	0.1066	0.0142
Skew interest rates (mean)	0.0251	1.6010	0.6978	0.5295
Corr(density,stability)	-0.4688	-0.3837	-0.7981	0.0275
Corr(density,rates)	0.0296	0.0896	0.7960	0.0229
Autocorr(density)	0.0034	0.2455	0.8174	0.0243
Autocorr(avg volume)	0.0014	0.0760	0.4926	0.0555
Autocorr(avg rate)	0.9991	0.2425	0.9655	0.0031
Objective function value	227.3328	4.2407		
Euclidean norm $\Vert\hat{\boldsymbol{\beta}}_T - \tilde{\boldsymbol{\beta}}_{TS}\Vert$	6.8563	2.0035		
Sup norm $\Vert\hat{\boldsymbol{\beta}}_T - \tilde{\boldsymbol{\beta}}_{TS}\Vert_\infty$	4.4568	0.9032		

[a] Not included in auxiliary vector as proportional to average degree.

the observed counterparts of 1.8 and 1.6. These network characteristics can be attributed to the structure of liquidity shocks across banks and asymmetric information problems about counterparty risk and search frictions, as discussed in the next section. Indeed, the calibrated parameter $\boldsymbol{\theta}_a$ parametrized a setting where counterparty risk uncertainty is more equally distributed in the cross-section due to the absence of monitoring.

Second, and key to our analysis, the estimated structural model is able to generate patterns of relationship lending where banks repeatedly interact with each other and trade at lower interest rates. In particular, the positive correlation of 0.60 between past and current bilateral lending activity, that measures the stability of bilateral lending relationships, matches well the observed value of 0.64. Moreover, the model generates a negative correlation of interest rates and past trading of -0.12 (as compared to -0.07 for the observed data). As reported in Table 3 monitoring efforts positively depend on the expectation about being approached by a specific borrower. Once a contact between two banks is established, banks positively adjust their expectation and increase monitoring. This has dampening effects on the bilateral interest rate level and thereby further attracts the borrower leading to yet increased expectations about a contact. The role of counterparty selection and monitoring as crucial drivers behind the observed dynamic structure of the interbank market is also confirmed by comparing the fit of the auxiliary statistics simulated under the calibrated parameter with those of the estimated parameter. Clearly, under the calibrated example where there is no role for monitoring bilateral stability is low (0.23) and there is no effect of past trading on current prices.

Moreover, we see that our model is able generate quite some autocorrelation in the density (0.25) and the average interest rate of traded loans (0.24). Clearly, the estimated values are not as high as the observed (0.81 and 0.97, respectively). However, note that there are no common factor in the model and all shocks are iid. Hence, the generated autocorrelation in aggregate figures results from the same banks being in the market in adjacent periods. Similar, we also generate a negative correlation between the density and the stability and a positive correlation between density and average spreads. Finally, we note also that the model does a poorer job in explaining the observed average interest rate level. This partly reflects the fact that the model abstracts from time-varying outside options for lending and borrowing that are, for instance, associated to massive central bank interventions during the financial crisis. Further, the skewness of the cross-sectional interest rate distribution is over-estimated and the variance of the traded volumes is too low. Recall that the model abstracts from any bank heterogeneity beyond differences in liquidity shocks, in particular differences in balance sheet strength or heterogeneous outside options.

5 Model Analysis

One of the most appealing features of structural models is the possibility to answer meaningful economic questions and derive relevant policy implications. As we shall now see, the estimated structural model described above can be used not only to study the effects of key frictions on the network structure, but also, as an interesting testing ground for different policies affecting the interbank lending market. Here we focus on assessing the role of private information, gathered through monitoring and repeated interaction, in reducing asymmetric information problems about counterparty risk.

5.1 Topology of the Interbank Network

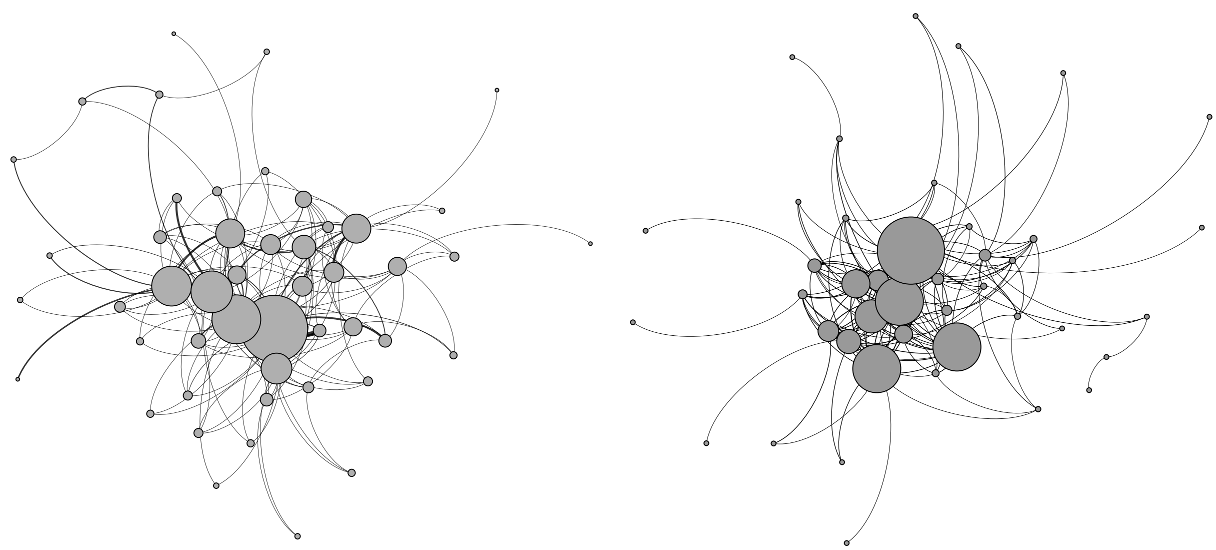

(a) Observed network (b) Simulated network

Figure 3: Interbank network during one week. Nodes are scaled according to total trading volume. Observed network corresponds to first week in April 2008. Simulated network is randomly picked realization. Figures made with Gephi (Yifan Hu).

Figure 3 depicts the observed interbank network along with a network simulated from the estimated model based on interbank lending activity during five trading days. Both the observed and simulated lending network are sparse and lending is highly concentrated. In particular, both networks are characterized by few banks in the center of the network which trade large volumes on either side of the market (scale of nodes relates to volume). On the other hand the majority of banks trades small values or is not participating in the market at all on a weekly frequency. The visualization also highlights the skewed degree distribution of the observed and simulated network. In particular, large banks in the core have multiple counterparties, while small banks typically have few trading partners and they are typically connected with banks in the center.

Figure 4 plots the simulated (marginal) in-degree and out-degree distribution under the estimated model parameters. The figure is the results of a MC analysis based on 5000 different networks each with T = 25. About 65% of all banks have zero trading partners on a daily basis (isolated vertexes), i.e. they do not lend or borrower in the market. Moreover, the majority (about 60%) of active banks has at most two borrowers and lenders. At the same time both degree distributions have a very long right tail indicating that there are few banks that borrow and lend from many other banks. Yet banks that have more than ten counterparts on a daily basis are very rare with relative frequency below 1%.

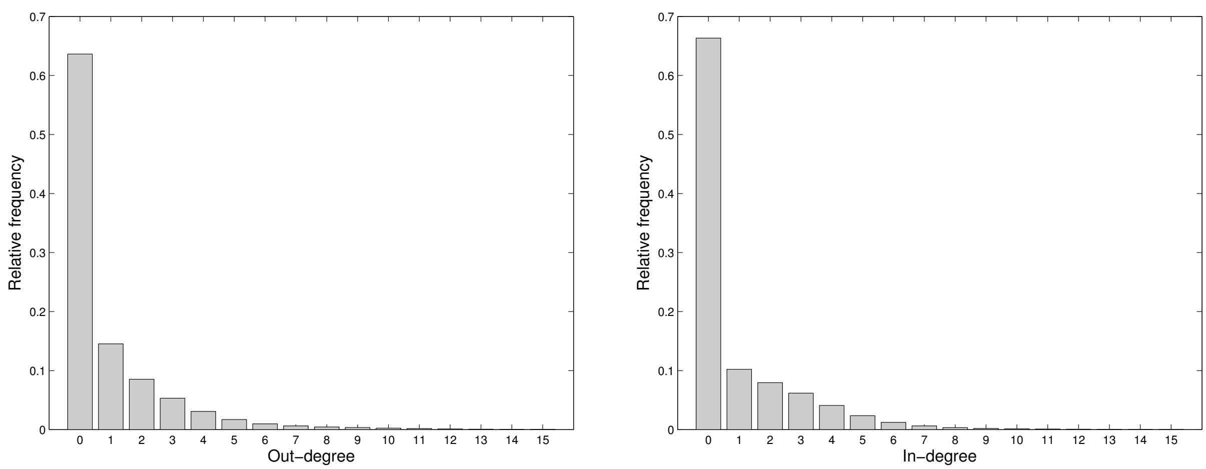

(a) Out-degree distribution

(b) In-degree distribution

Figure 4: Marginal in-degree and out-degree distribution based on 5000 simulated network paths of size T = 25 under the estimated parameter vector.

The estimated model allows us to directly relate key network properties to structural parameters that are linked to clear economic concepts, in particular credit risk uncertainty and peer monitoring. Figure 5 graphs how the mean density, reciprocity, skewness of out-degree and in-degree distribution, mean monitoring and mean search respond to changes in structural parameters by +/- 10% from their estimated values. Specifically, we focus on varying the coefficient of monitoring ($\beta_{\phi,1}$) in Equation (3), the autoregressive coefficient of the log perception error variance (γ_σ) in Equation (1) and the parameter that determines the location of the logistic link probability function (α_λ) in Equation (5), while holding constant all other parameters at the estimated values.

The left panel shows that an increase in the persistence of the log perception error variance leads to a lower network density and a higher fraction of reciprocal lending relationship. Moreover, for the plotted range of values of γ_σ, both the in- and out-degree skewness exhibits

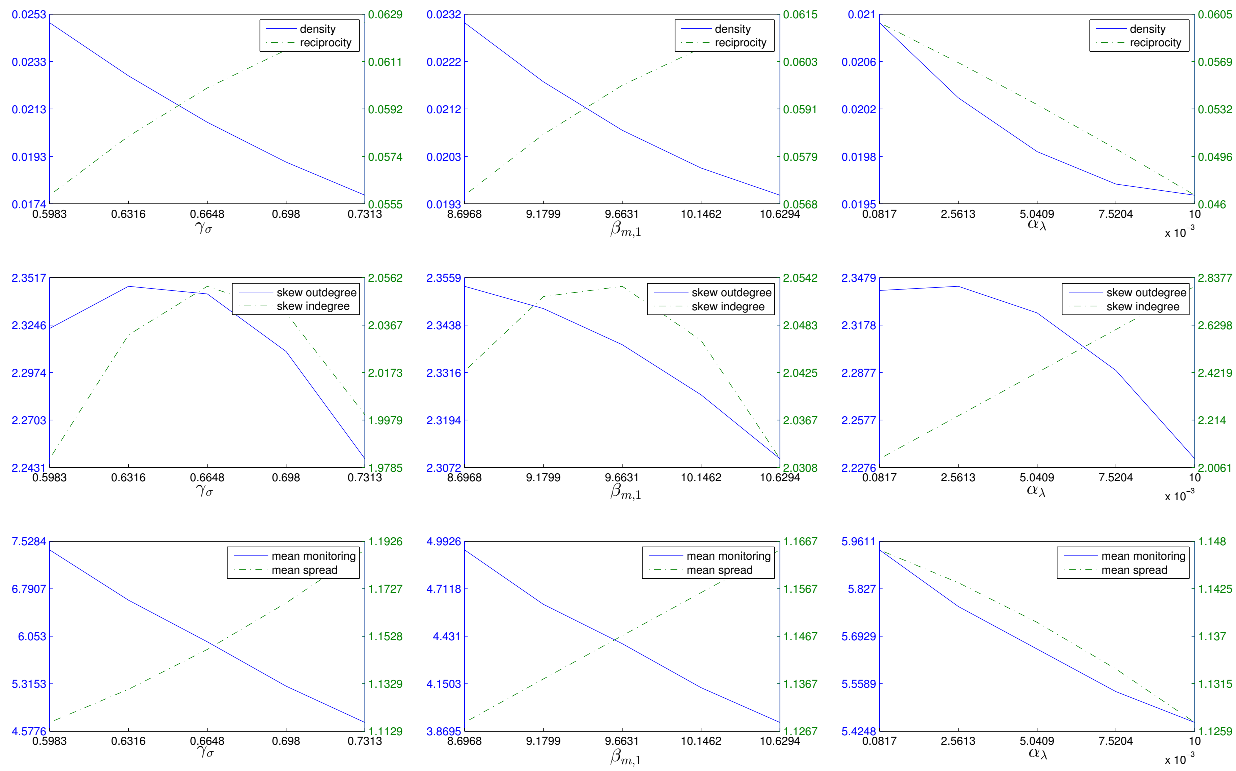

Figure 5: Comparative statics of network statistics. Simulated mean of network statistics as a function of key structural parameters related to credit risk uncertainty (γ_σ), efficacy of peer monitoring ($\beta_{m,1}$), and search frictions (α_λ). Parameters range from +/-10% around estimated values, holding fix all other parameters. Each graph is based on 5000 MC repetitions each with T=500. Left (right) axes correspond to solid (dashed) lines.

a hump shaped form. For a low persistence in credit risk uncertainty an initial increase in γ_σ leads to higher skewness of the degree distributions, in particular the in-degree becomes more asymmetrically distributed. Economically, as the persistence of credit risk uncertainty increases some banks lose trading partners – potentially not accessing the market at all – while borrowing concentrates on few highly connected banks that can still maintain sufficiently many lending relations. As the uncertainty increases further, however, lender banks will also occasionally refrain from providing credit to these money center banks and the skewness decreases again. Moreover, a more persistent uncertainty leads to higher spreads of granted loans and decrease monitoring efforts.

From the middle panel we see that the network shows a qualitatively similar response to an increase in the marginal effect of monitoring on the added information, in particular the density decreases and lending become more reciprocal. At the same time the average spread of granted loans increases and banks on average reduce peer monitoring efforts (bottom plot). The decline in monitoring occurs because $\frac{\partial \pi_{i,t}}{\partial m_{i,j,t} \partial \beta_{\phi,1}}|_{\theta=\hat{\theta}} < 0$ for sufficiently large

$m_{i,j,t}$, in particular at the expansion point of the FOCs. Intuitively, banks steady state monitoring levels are such that uncertainty is already relatively low and an increase in $\beta_{\phi,1}$ further reduces the marginal benefit from monitoring. To maintain the equality between the (constant) marginal cost and benefit a reduction in monitoring is necessary.

The right panel reveals that if banks need to invest more to maintain the same link probability, less trade occurs and lending becomes less reciprocal because some banks will not find it profitable to maintain some of their trading relationships. However, as the large increase in the in-degree skewness suggest, the reduction in lending partners at the borrower level is again asymmetrically distributed. In particular, as the cost of link formation increases borrowing becomes more concentrated towards few highly connected core banks. At the same time the reduction in out-degree skewness is the result that highly connected lenders lose some of their borrowers that don't find it profitable anymore to incur the search cost, thereby reducing the asymmetry of the degree distribution. Moreover, while the average monitoring expenditures decrease as a reaction to higher cost of linking, the mean spread of granted loans decreases because those bank pairs that continue trading have lower uncertainty about their counterparts.

5.2 Bank Heterogeneity and Lending Relationships

Heterogeneous liquidity shock distributions are crucial in matching the basic network structure of the interbank market, such as the high skewness of the degree distribution and the emergence of trading relationships. In our model the distribution of liquidity shocks in the banking system in characterized by the probabilistic structure described in Section 3.

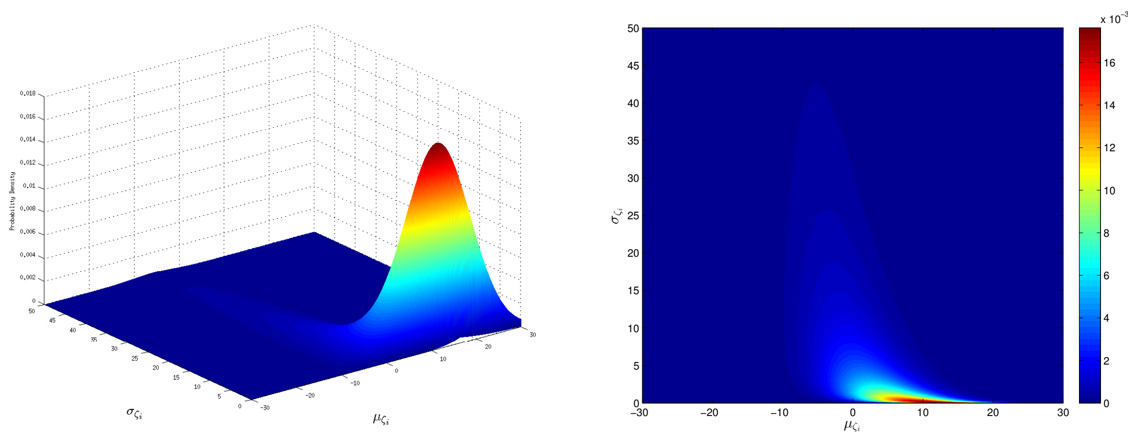

(a) Density (b) Contour plot

Figure 6: Joint distribution of mean (μ_{ζ_i}) and standard deviation (σ_{ζ_i}) of banks' liquidity shock distributions and contour plots as implied by the estimated model parameters.

Figure 6 plots the joint distribution of the bank specific mean μ_{ζ_i} and standard deviation σ_{ζ_i} of the liquidity shocks as implied by the estimated structural parameters $\hat{\mu}_\mu = 0$, $\hat{\sigma}_\mu = 1.99$, $\hat{\mu}_\sigma = 1.94$, $\hat{\sigma}_\sigma = 1.98$ and $\hat{\rho}_\zeta = -0.78$. First, note that most probability mass is located around $\mu_{\zeta_i} = 0$ and at small values of σ_{ζ_i}. Hence the median bank has small liquidity shocks that are about zero on average. Second, the distribution of μ_{ζ_i} is more dispersed for low values of σ_{ζ_i}. Thus for banks with a small variance parameter of the liquidity shock distribution (small banks) there is a higher heterogeneity with respect to their mean parameter μ_{ζ_i}. Third, the contour plot reveals a banana shaped form of the distribution. In particular, small banks with very small-scaled liquidity shocks typically tend to have a liquidity surplus, while banks with very large-scaled shocks typically have a negative mean, indicating a liquidity deficit. This relation is driven by the correlation parameter ρ_ζ that we estimate to be -0.78. Finally, note the long tail in the dimension of σ_{ζ_i} shows that few banks feature very large liquidity shock variances.

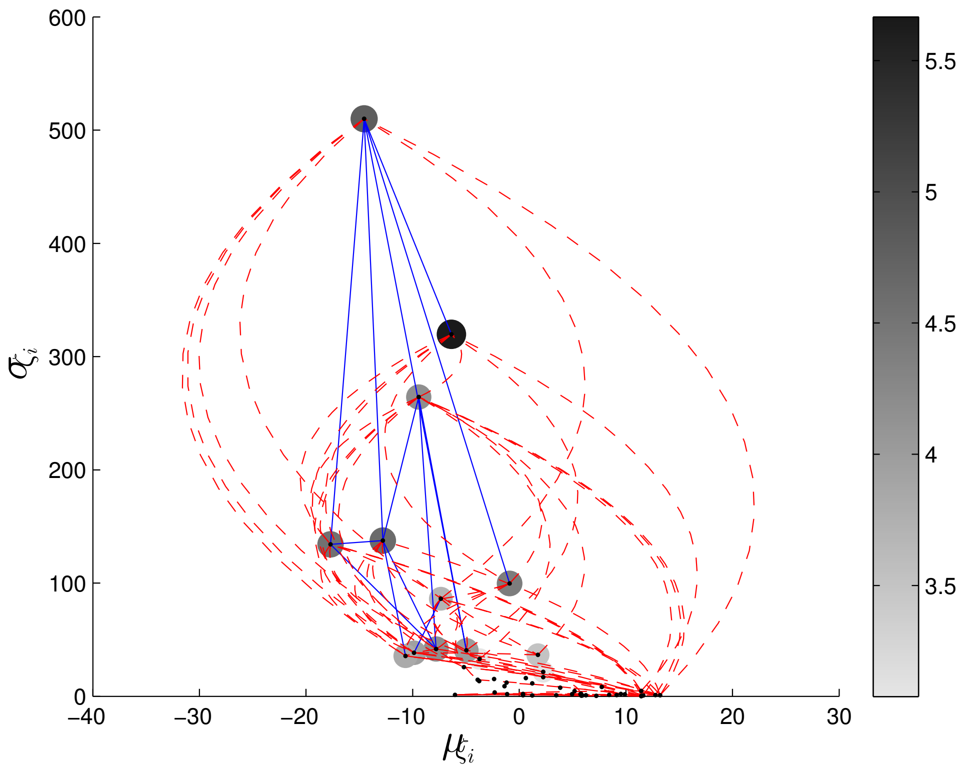

Figure 7: Simulated interbank network (5 trading days). Banks position in μ_ζ-σ_ζ plane given by mean and standard deviation parameter $(\mu_{\zeta_i}, \sigma_{\zeta_i})$. Node size scaled proportional to average loan volume per bank. For each node incoming links are shown as dashed red lines coming from the right, outgoing links leave nodes from the left (counterclockwise). Solid blue lines represent reciprocal links.

The estimated bank heterogeneity has important consequences for pairwise credit availability and conditions as well as on search and monitoring expenditures. In Figure 7 we graph the interbank activity during one week (five days) for 50 randomly drawn liquidity shock parameters (associated with 50 banks). Each bank is indicated by a black dot and its position in the μ_ζ-σ_ζ plane is given by the values of the bank specific mean and standard deviation parameters $(\mu_{\zeta_i}, \sigma_{\zeta_i})$. The node size around each dot is scaled proportional to the total degree of each node (bank). Moreover, for each node outgoing links leave nodes from the left (counterclockwise) and solid blue lines represent reciprocal links, that is links that connect two bank where both banks act as lender and borrower to each other. The figure reveals that small banks (small liquidity shock variance) are typically providing liquidity to the market, in particular to big banks (those that on average have a positive demand for liquidity) or small banks with complementary liquidity shocks. This results is in line with similar empirical findings by Furfine (1999) and Bräuning and Fecht (2012) that small banks are net lenders. In the market intermediation emerges as big banks (money center banks) act as lenders and borrowers at the same time. For small banks it is most efficient to trade with big banks that have large liquidity shocks than with banks with small ones. Moreover, big banks form a tightly inter-connected core where each member of the core has reciprocal lending relationships (solid blue lines) with other core banks, see the core-periphery analysis by Craig and von Peter (2014) and van Lelyveld and in 't Veld (2012). Clearly, big banks trade on average larger loan volumes than small banks as a results to their larger-scaled liquidity shocks.

We next present more rigorous Monte Carlo evidence to analyze the link between bank heterogeneity as the fundamental source of persistent trading opportunities that is reinforced by the interrelation between credit risk uncertainty, peer monitoring and counterparty search. For this purpose, we simulate 5000 network paths and sort for each draw the lender banks according to their variance parameter σ_{ζ_i} and the borrower banks according to their mean parameter μ_{ζ_i} in increasing order. Hence, we compute the order statistics of both parameters. We then simulate for each draw $T = 25$ periods and compute the mean link probability, mean volume and spreads of granted loans as well as mean search and monitoring efforts between the lender order statistics and the borrower order statistic of all possible bank pairs.

Panel (a) in Figure 8 depicts the mean granted loan volumes for different bank pairs. In particular, we see that banks with a structural liquidity deficit (on the left of the horizontal axis) are borrowing larger loan amounts than banks with a structural liquidity surplus (on the right of the horizontal axis). Both type of banks borrow larger volumes from big banks with a large variance parameters (on the top of the vertical axis). Due to the negative correlation parameter ρ_ζ, bank with low order statistic $\mu_{\zeta_{(i)}}$ are typically big banks and thus

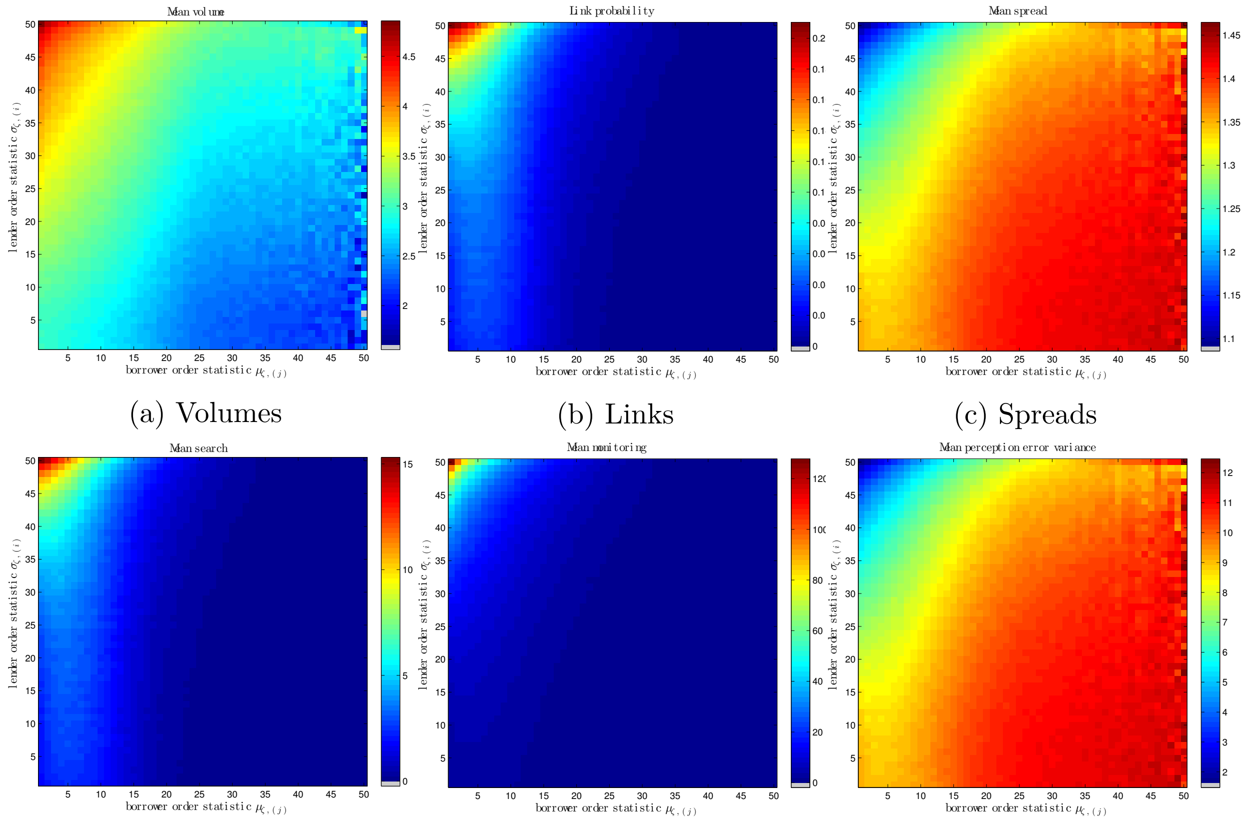

(a) Volumes (b) Links (c) Spreads

(d) Search (e) Monitoring (f) Uncertainty

Figure 8: Bank heterogeneity and trading relationships. The order statistics of lender variance parameters $\sigma_{\zeta_{(i)}}$ is depict on vertical axis, order statistics of borrower mean parameter $\mu_{\zeta_{(i)}}$ is depict on horizontal axis, i.e. lender banks are ordered by variance parameter σ_{ζ_i} such that $\sigma_{\zeta_{50}} > \sigma_{\zeta_{49}} > ... > \sigma_{\zeta_1}$ and borrower banks ordered by mean parameter such that $\mu_{\zeta_{50}} > \mu_{\zeta_{49}} > ... > \mu_{\zeta_1}$. Results based on 10000 MC repetitions, each of length T=100.

borrowing volumes with other big banks (with large $\sigma_{\zeta_{(i)}}$) are high. Similarly, mean traded volumes are low for banks with a structural liquidity surplus and lender banks with a small scaled variance parameter see the blue region in panel (a).

In panel (e) we see how the distribution of loan volumes affects monitoring decisions that eventually affect the prices at which bank pairs trade liquidity, see panel (c) and (e). Those bank pairs that can exchange large loan amounts (either because they have large variance or because they have complementary shocks) monitor more and trade at lower spreads, see the banana shaped contour plots. Again we see that the very large banks have very high monitoring efforts and trade at very low rates with each other (up to 40 bps lower than high spread pairs). Hence, these core banks are not only highly interconnected but also credit risk uncertainty among these banks is very low, see panel (f). Due to the interrelation with monitoring and search low interest regions in the graphs correspond to bank pairs where search levels are high and this leads to high link probabilities, see panel (b). Moreover, borrowers with a structural liquidity deficit obtain larger volumes at lower prices when borrowing from large banks than from small banks. This further highlight the role of intermediation in the model. Intermediaries have less credit risk uncertainty about their borrowers due to higher monitoring intensities, and in turn borrowers have lower credit risk uncertainty about intermediary banks because lenders channel monitoring towards those banks. Hence, the network's tiered structure that results from differences in liquidity shocks is reinforced by the presence of credit risk uncertainty and peer monitoring.

5.3 Dynamic Responses to Credit Risk Uncertainty Shocks

In this section, we analyze the effect of shocks to the perception error variance on the dynamics the estimated network model. To account for the uncertainty about the precise latent liquidity shock distributions we perform a simulation study by first drawing the bank properties (as described by the parameters μ_{ζ_i} and σ_{ζ_i}) and then calculating a set of key network statistics for T = 25 time periods. This procedure was then repeated in a Monte Carlo setting with 5000 replications. In all simulated structures we impose a large positive shock to the perception error variance in period $t = 4$ (affecting the perception error variance in $t = 5$) to investigate how our key network statistics react to increases in credit risk uncertainty.

The solid lines in Figure 9 depict the mean responses across all network structures to a extreme ten standard deviation shock in credit risk uncertainty, i.e. we impose $u_{i,j,4} = 10\ \forall i, j$. The interquartile range (dotted lines) in this figure reflects essentially the uncertainty about the exact network structure as described by the unobserved liquidity shock distributions. For instance, the interquartile range of the mean network density is between 0.014 and 0.023 and the mean is about 0.019 depending on the precise network structure as already discussed. In the top panel, we see that at the time of the shock to the credit risk uncertainty the network density drops by more than 75%. Both density and total volume remain at low levels and twenty trading days after the shock they are still at 50% of their pre-crisis value. Moreover, the log of total transaction volume plummets by more than 50% as a result of less trading activity. At the same time we observe an increase in the average (log) volume of granted loans compared to pre-shock levels and an increase in the network stability one period after the shock. Similarly, both in-degree and out-degree distribution become more positively skewed and the reciprocity increases more than twofold (the lower bounds remains at zeros because for some network structure interbank lending breaks down completely leading to zero reciprocity). Hence, the network shrinks and trading becomes more concentrated

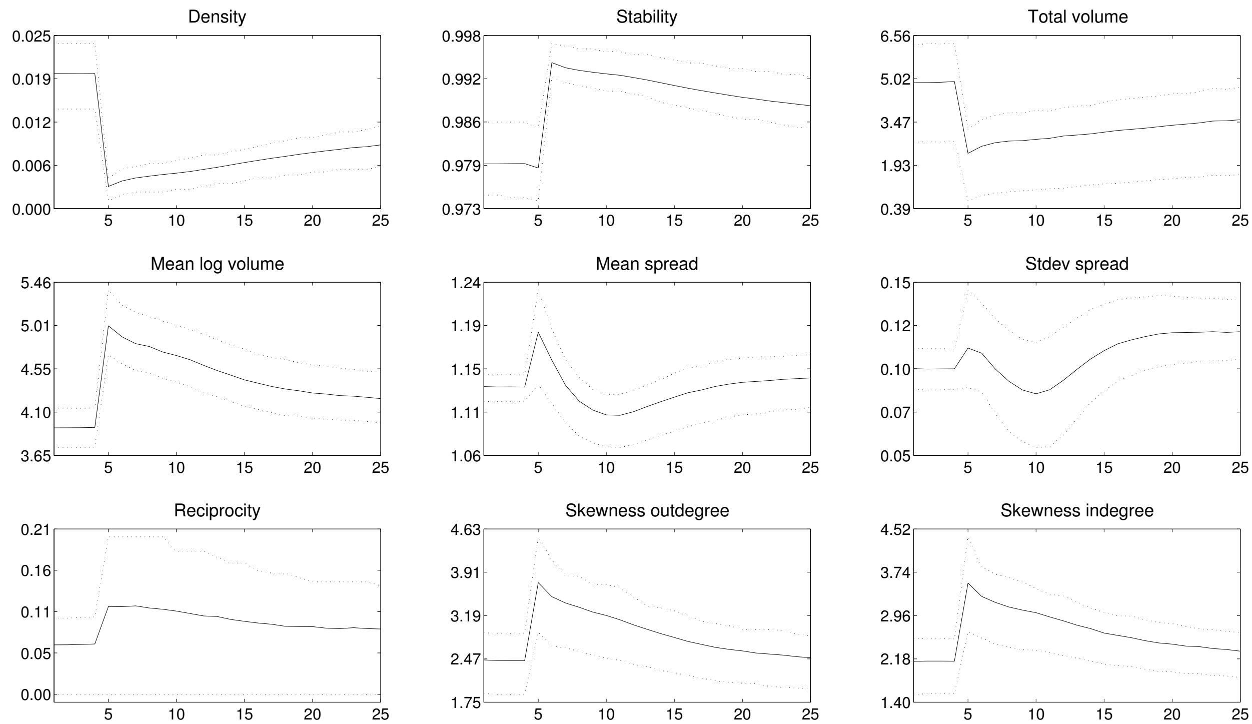

Figure 9: Simulated impulse responses to a common ten standard deviations shock in credit risk uncertainty in t = 4. Results are based on 5000 MC repetitions. The solid line is the mean impulse response, the dotted lines refer to the interquartile range across all network structures. Total volume is in billions and mean volume is the mean log volume (in millions) of granted loans.

among highly interconnected core banks.

These changes are driven by the fact that some bank pairs that are active before the shock, stop trading as the lenders' risk assessments impair, implied interest rate spreads explode and are for some pairs too high compared to the outside option. These loans are substituted by increased recourse to the central bank's standing facilities (not shown) which moves inversely to the density and total transaction volume. In fact, the increased average loan volume shows that in period t=5 relatively more bank-pairs are active that exchange larger volumes (due to their size and/or complementarity of liquidity shocks). As discussed in the previous section, these are bank pairs where monitoring is particularly profitable and bank-to-bank uncertainty is low making interbank lending still more attractive than the outside option even after the shock hit. Yet, also those trades that do occur are associated with increased spreads due to higher uncertainty such that the average spread of granted volumes increases by about 6 bps right after the shock. The compositional effects, do hence not immediately outweigh the uncertainty induced increases of interest rates. However, about two periods after the shock, the average spread of trades that do occur are back to initial levels and a further decrease can be observed until about period 10 when the average rate of traded loans is below the level before the shock. A similar pattern can be observed for the cross-sectional standard deviation of interest rates. While it increases to 0.11 as the shock hits, it decreases to about 0.09 in period 10 when mean spreads are lowest and then increases to levels higher than before the shock for an extended period of time.

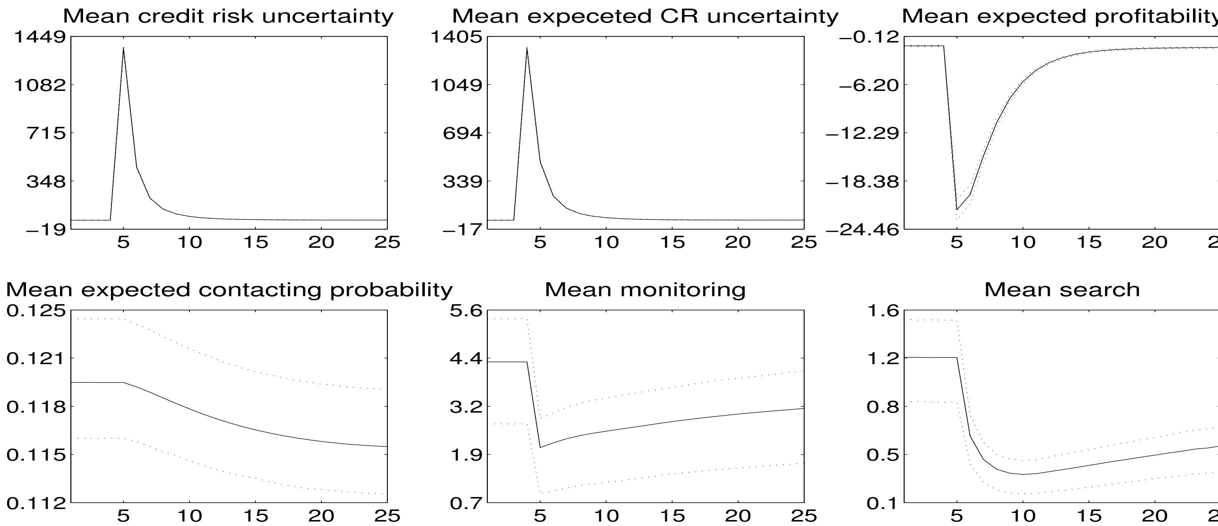

Figure 10: Simulated impulse responses to a common ten standard deviations shock in credit risk uncertainty in t = 4. Results are based on 5000 MC repetitions. The solid line is the mean impulse response, the dotted lines refer to the interquartile range across all network structures. Expectations are in deviations from steady state values. Monitoring and search expenditures are in thousands of euros.

Figure 10 depicts the impulse responses for the banks' expectations and control variables as crucial drivers behind the discussed changes in observable network statistics. Again the solid line refers to the mean and the dotted lines to the inter-quartile range representing the uncertainty about the latent network structure. The top left panel shows how mean credit risk uncertainty peaks at the time of the shock in period t=5. Clearly, the increase in mean credit risk uncertainty translates into an increase in the mean expectations about future credit risk uncertainty that show a similar behavior yet at lower values. As a consequence of the higher (expected) uncertainty (that is directly translated into higher bilateral equilibrium rates) after the shock the expected profitability of interbank borrowing decreases as the spread that can be earned compared to discount window borrowing declines. This leads borrower banks to invest less into counterparty search further bringing down interbank trade. Note that the impaired funding conditions due to higher credit risk uncertainty only feed gradually into borrower's expectations about interbank profitability, as banks only update their expectations once they got in contact with a lender. Therefore, mean search effort decline gradually until they reach a minimum in period 10. Moreover, these lower search efforts are picked up by lenders' expectations about future contacting probabilities that gradually decline from period 5 onwards until the end of the plotted sample (though the decrease in the mean expectation is arguably small).

Moreover, as a response to the increased perception error variance banks adjust their monitoring expenditures from about on average 4.5 thousands euros (per bank-pair) downwards to 2 thousands euros. Several channels drive this decease that contributes to the prolonged decline in interbank trading activity and prevents a fast recovery of the market. As can be seen from the estimated linear policy rules, the higher credit risk uncertainty makes monitoring more profitable, however at the same time adjustments to future expected uncertainty make monitoring less profitable. Because the estimated EMWA forecast parameter is low, these expectations follow closely the actual credit risk uncertainty that has quite persistent dynamics. In sum, the negative effect of future uncertainty dominates such that the overall mean effect of this large three standard deviations shock is negative. In addition, the gradual decrease in expected future contacting probability due to lower search efforts further dampens bank's monitoring expenditures and prevents a faster recovery of the market. Note, that we plot here the mean values of bank-to-bank specific expectations and control variables. Of course, other moments change as well as a response to the shock, in particular the distribution of monitoring and search efforts becomes more skewed.

In Figure 11, we analyze heterogeneous responses to a shock in credit risk uncertainty. To this end we group for each MC repetition banks into three categories based on total trading volume during the 100 periods preceding the shock it t = 4. Group 1 includes the largest 5 banks in terms of total trading volume (1th-10th percentile), group 2 includes the 6th to 25th (11th-50th percentile) and group 3 includes the remaining banks (51th-100th percentile). In the top left panel, we see that the large banks have on average a much higher link probability than the medium sized or small ones. In fact, the latter group has a very low participation rate close to zero. As with respect to the dynamics after the shock, we observe a drop in trading activity for big and medium sized banks and a subsequent increase with a similar pattern as for the aggregate figures. For the small banks that are mostly inactive anyway, there is no effect of the shock.

In the top right panel we plot the mean interest rate spreads for the three groups. Large banks trade at spreads of about 1.10 % while medium sized banks pay about 1.16 %. For small banks the mean spread of granted loans is by about 25 basis points higher with average values of 1.40 %. Interestingly, we see a heterogeneous reaction to the shock. The spreads big and medium banks pay increase as a response to higher uncertainty, for big banks however the increase is only about 5 bps whereas for big banks it is about 10 bps. On the other

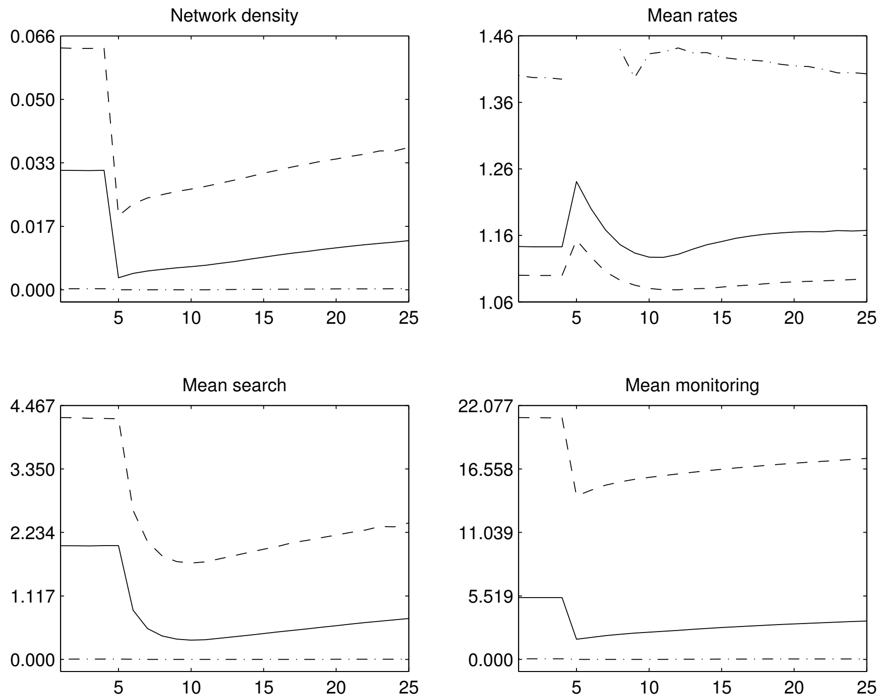

Figure 11: Heterogeneous impulse responses of top 5 (dashed line), 6-25 (solid line), 26-50 banks (dashed-dotted line) in terms on total volume in 100 periods preceding the common ten standard deviations shock to credit risk uncertainty in t = 5. Simulation results based on 5000 MC repetitions.

hand, small banks completely stop borrowing in the market for three periods as the shock hits. Because the spread those banks is already very high a slight increase in uncertainty will lead to bilateral rates that are outside the corridor and banks will not settle a deal.

5.4 Monetary Policy Analysis: The Interest Corridor Width Multiplier

The width of the central bank's interest rate corridor is a key parameter of the model as it provides the outside option of interbank lending. In this section, we analyze how changes in the width the corridor affect the interbank lending network and associated credit conditions. In particular, we show that monetary policy has a direct influence on interbank lending and an indirect effect as it changes banks' monitoring efforts.

Figure 12 shows how the width of the ECB corridor produces significant changes in the structure of the interbank lending network that is driven by changes in banks' monitoring and search efforts. Again, the uncertainty captured by the interquartile range captures to a large extent the uncertainty about the precise latent distribution of liquidity shocks in the banking system. The most striking feature of Figure 12 is that an increase of roughly

100% in the width of the ECB's interest rate corridor (from 1 to 2) produces a more than threefold increase in the mean network density (average number of daily trades) from roughly 1% density to over 3%. Furthermore, at a corridor width of 2%, the lower bound of the interquartile range across all network structures is larger than the upper bound on the interquartile range across network structures at a corridor width of 1%. This analysis shows that these effects are highly significant and that the ECB corridor width plays an important role in the intensity of interbank activity.

A second important feature of Figure 12 is that, since the model is nonlinear, the multiplier value is not constant over the range of ECB corridor widths. In particular, Figure 12 shows that the multiplier value is decreasing with corridor width. Indeed, a 0.1 unit increase on the bound has a much larger relative effect in density for low corridor widths compared to large ones. For instance, increasing the bounds from 1 to 1.25 leads to an increase in density by about 45%, while an increase from 1.75 to 2 leads to an increase of about 28%. The presence of this multiplier, as well as its nonlinearity, are both explained by the role that monitoring and search efforts play in the interbank market. Just like in the usual Keynesian multiplier, the effects of a change in the width of the ECB bounds can also be decomposed into *(i)* an immediate short-run effect, and *(ii)* a long-run effect that is created by the multiplier that results from feedback loops between the effect of monitoring and search on loan outcomes and expectations about credit conditions.

Consider a decrease in the width of the ECB corridor. In the advent of such a shock, the interbank market will immediately shrink as a fraction of lending and borrowing operations are no longer profitable given the new tighter ECB bounds. In this immediate 'mechanical' effect, part of the interbank market is simply 'substituted' by lending and borrowing with the central bank authority which now plays a more important role. This immediate short-run effect is however only a fraction of the total long-run effect. Indeed, given that the possibilities of trade are now smaller, the expected future profit is diminished and the incentive to monitor and search partners is reduced. This reduction is monitoring and search (depicted in Figure 12) will further reduce the mean density and mean traded volumes in the interbank market. These, in turn force banks to revise the expected profitability of monitoring and search efforts, pulling these variables further down. This 'negative spiral' that defines the multiplier will bring the market to a new level of operation that can be orders of magnitude lower than that observed prior to the bounds.

Moreover, from Figure 12 we see that with a larger interest corridor both the mean spread of granted loans (to center of the corridor) as well as the cross-sectional standard deviation increases, while the average (log) volume traded decreases. The changes in these market outcomes are driven by bank pairs that did not trade under the narrower interest rate

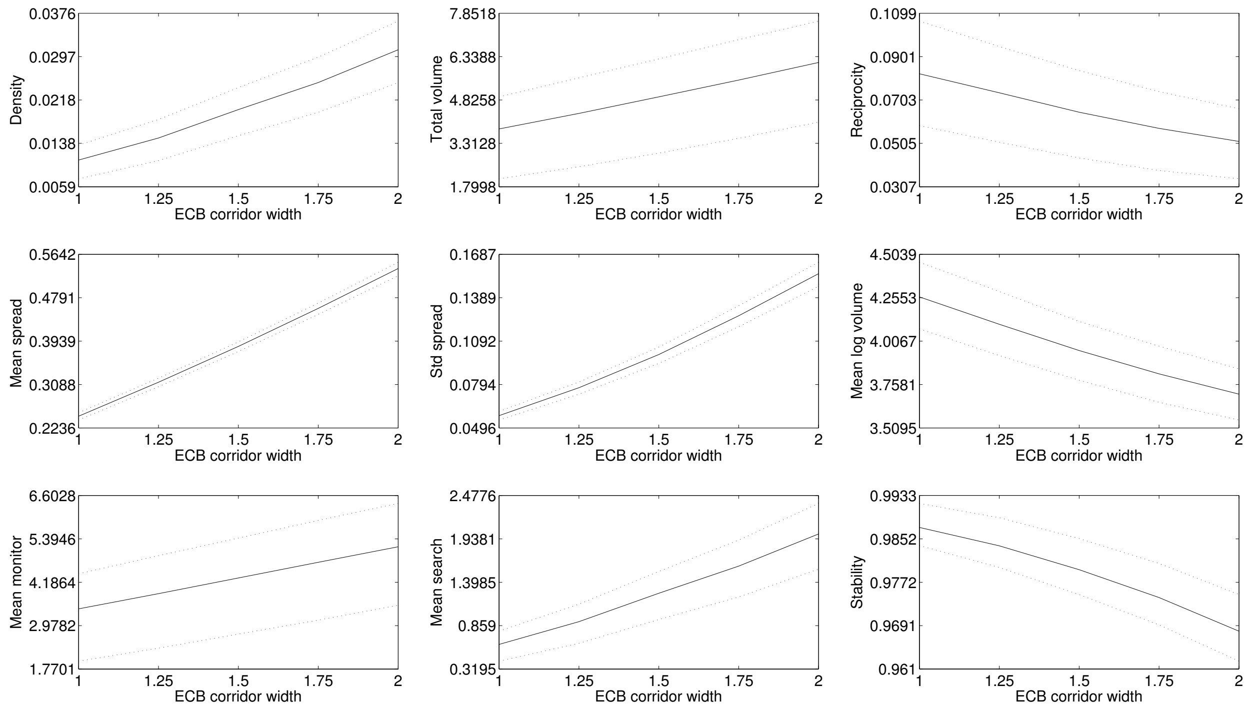

Figure 12: Simulated mean and inter-quartile range of key network statistics and mean monitoring and mean search per bank over alternative ECB interest corridor width. Total volume is in billion euros. MC results based on 5000 networks each with $T = 25$.

corridor but preferred to deposit funds at the central bank. After the increase of the corridor for those bank pairs trading becomes profitable, though interest rates are still high driving up the average rate and standard deviation of granted loans. Similarly, the reciprocity of the trading network and the stability decreases because with a wider corridor trading becomes more attractive for banks that only occasionally access the market.

Hence, if the ECB wishes to get tighter control over the traded rates by narrowing the corridor it has to expect further adverse effects on interbank lending activity triggered by a reduction of monitoring and search. On the other hand, if the ECB wants to foster an active decentralized interbank lending market as a means to explore benefits from peer monitoring it is essential to consider policies that increase the difference between the standing facilities for depositing and lending funds. Only thereby the interbank market is profitable enough to encourage intense peer monitoring and search among banks. In both cases the multiplier effect should be taken into account when considering policy changes.

6 Conclusion

In this paper we propose and estimate a structural micro-founded network model for the unsecured interbank lending market where banks can lend and borrow funds in an over-the counter market to smooth liquidity shocks or resort to the central bank standing facilities. Therefore they choose which counterparties to approach for bilateral Nash bargaining about interest rates and set monitoring efforts to mitigate asymmetric information problems about counterparty risk. The optimal search and monitoring levels are characterized as functions of the expected profitability of bilateral interbank transactions.

We estimate the structural model parameters using loan level data at daily frequency collected for the Dutch unsecured overnight interbank lending market from 2008 to 2011. Our results show that prevailing bank-to-bank uncertainty and peer monitoring can generate key characteristics of interbank markets. First, banks form long-term lending relationships that are associated with improved credit conditions. Second, the lending network exhibits a sparse core-periphery structure. Moreover, our dynamic analysis shows that shocks to credit risk uncertainty can bring down lending activity for extended periods of time.

Moreover, we use the estimated model to discuss monetary policy implications. In particular, we show that in order to foster the trading activity in unsecured interbank markets and associated benefits from peer monitoring an effective policy measure is to widen the bounds of the interest corridor. The effects of a wider corridor result from both a direct effect and a non-linear, indirect multiplier effect triggered through increased monitoring and search activity among banks serving as a leverage to monitoring policy.

For future research, we believe that our framework could be used to study several interesting extensions. First we could allow banks holding reserves on the central bank account, to study effects of liquidity hording and excess liquidity on market participation and interest rate.[16] Second, this paper leaves open the question of the optimal corridor size, which requires assumptions about the central banks preferences see for instance Bindseil and Jabłecki (2011). Third, an interesting analysis could ask how the failure of an interbank relationship lender that disposes of private information tightens credit conditions for its respective borrowers, thereby giving room to contagion from the asset side.

References

Abbassi, P., Gabrieli, S., and Georg, C.-P. (2013). A network view on money market freezes. Technical report, mimeo.

[16] In this paper, we do for instance not address the effects of the LTROs as of end 2011.

Acemoglu, D., Ozdaglar, A., and Tahbaz-Salehi, A. (2013). Systemic Risk and Stability in Financial Networks. NBER Working Papers 18727, National Bureau of Economic Research, Inc.

Acharya, V. V. and Merrouche, O. (2013). Precautionary Hoarding of Liquidity and Interbank Markets: Evidence from the Subprime Crisis. *Review of Finance*, 17(1):107–160.

Affinito, M. (2011). Do interbank customer relationships exist? and how did they function over the crisis? learning from italy. Systemic risk, basel iii, financial stability and regulation 2011, Bank of Italy.

Afonso, G., Kovner, A., and Schoar, A. (2011). Stressed, not frozen: The federal funds market in the financial crisis. *Journal of Finance*, 66(4):1109–1139.

Afonso, G., Kovner, A., and Schoar, A. (2013). Trading partners in the interbank lending market. Staff Reports 620, Federal Reserve Bank of New York.

Afonso, G. and Lagos, R. (2012). Trade dynamics in the market for federal funds. Staff Reports 549, Federal Reserve Bank of New York.

Alatas, V., Banerjee, A., Chandrasekhar, A. G., Hanna, R., and Olken, B. A. (2012). Network Structure and the Aggregation of Information: Theory and Evidence from Indonesia. Working Papers id:5106, eSocialSciences.

Allen, F. and Gale, D. (2000). Financial contagion. *Journal of Political Economy*, 108(1):1–33.

Arciero, L., Heijmans, R., Heuver, R., Massarenti, M., Picillo, C., and Vacirca, F. (2013). How to measure the unsecured money market? the eurosystem's implementation and validation using target2 data. DNB Working Papers 369.

Ashcraft, A. B. and Duffie, D. (2007). Systemic illiquidity in the federal funds market. *The American Economic Review*, 97(2):221–225.

Babus, A. (2013). Endogenous intermediation in over-the-counter markets. Working Paper Imperial College London.

Babus, A. and Kondor, P. (2013). Trading and information diffusion in OTC markets. CEPR Discussion Papers 9271, C.E.P.R. Discussion Papers.

Bech, M. L. and Atalay, E. (2010). The topology of the federal funds market. *Physica A: Statistical Mechanics and its Applications*, 389(22):5223–5246.

Bech, M. L. and Monnet, C. (2013). The Impact of Unconventional Monetary Policy on the Overnight Interbank Market. In Heath, A., Lilley, M., and Manning, M., editors, *Liquidity and Funding Markets*, RBA Annual Conference Volume. Reserve Bank of Australia.

Becher, C., Millard, S., and Soramäki, K. (2008). The network topology of CHAPS Sterling. Bank of England working papers 355, Bank of England.

Berentsen, A. and Monnet, C. (2008). Monetary policy in a channel system. *Journal of Monetary Economics*, 55(6):1067–1080.

Bindseil, U. and Jabłecki, J. (2011). The optimal width of the central bank standing facilities corridor and banks' day-to-day liquidity management. Working Paper Series 1350, European Central Bank.

Boss, M., Elsinger, H., Summer, M., and Thurner, S. (2004). Network topology of the interbank market. *Quantitative Finance*, 4(6):677–684.

Bougerol, P. (1993). Kalman filtering with random coefficients and contractions. *SIAM Journal on Control and Optimization*, 31(4):942–959.

Bramoullé, Y. and Fortin, B. (2009). The Econometrics of Social Networks. Technical report.

Broecker, T. (1990). Credit-worthiness tests and interbank competition. *Econometrica*, 58(2):429–52.

Bräuning, F. and Fecht, F. (2012). Relationship lending in the interbank market and the price of liquidity. Discussion Papers 22/2012, Deutsche Bundesbank.

Cocco, J. F., Gomes, F. J., and Martins, N. C. (2009). Lending relationships in the interbank market. *Journal of Financial Intermediation*, 18:24–48.

Craig, B. and von Peter, G. (2014). Interbank tiering and money center banks. *Journal of Financial Intermediation*, in press.

Cœuré, B. (2013). Exit strategies: time to think about them. Speech at the 15th geneva conference on the world economy, `http://http://www.ecb.europa.eu/press/key/date/2013/html/sp130503.en.html`, accessed: 2014-08-22.

de Frutos, J. C., de Andoain, C. G., Heider, F., and Papsdorf, P. (2014). Stressed interbank markets: Evidence from the European financial and sovereign debt crisis. mimeo.

DeJong, D. N. and Dave, C. (2006). *Structural Macroeconometrics*. Princeton University Press.

Diamond, D. W. and Dybvig, P. H. (1983). Bank runs, deposit insurance, and liquidity. *Journal of Political Economy*, 91(3):401–19.

Duffie, D., Garleanu, N., and Pedersen, L. H. (2005). Over-the-counter markets. *Econometrica*, 73(6):1815–1847.

Fagiolo, G. (2007). Clustering in complex directed networks. *Physics Review E*, 76:026107.

Farboodi, M. (2014). Intermediation and Voluntary Exposure to Counterparty Risk. Technical report, mimeo.

Freixas, X. and Holthausen, C. (2005). Interbank market integration under asymmetric information. *The Review of Financial Studies*, 18(2):459–490.

Freixas, X. and Jorge, J. (2008). The Role of Interbank Markets in Monetary Policy: A Model with Rationing. *Journal of Money, Credit and Banking*, 40(6):1151–1176.

Furfine, C. H. (1999). The microstructure of the federal funds market. *Financial Markets, Institutions & Instruments*, 8:24–44.

Furfine, C. H. (2001). Banks as monitors of other banks: Evidence from the overnight federal funds market. *Journal of Business*, 74:33–57.

Gai, P., Haldane, A., and Kapadia, S. (2011). Complexity, concentration and contagion. *Journal of Monetary Economics*, 58(5):453–470.

Gale, D. M. and Kariv, S. (2007). Financial networks. *The American Economic Review*, 97(2):99–103.

Georg, C.-P. (2013). The effect of the interbank network structure on contagion and financial stability. *Journal of Banking and Finance*, 77(7):2216 – 2228.

Gofman, M. (2014). Effciency and stability of a financial architecture with too-interconnected-to-fail institutions. mimeo.

Gourieroux, C., Monfort, A., and Renault, E. (1993). Indirect inference. *Journal of Applied Econometrics*, 8(S):S85–118.

Heer, B. and Maußner, A. (2005). *Dynamic general equilibrium modelling.* Springer, Berlin.

Heider, F., Hoerova, M., and Holthausen, C. (2009). Liquidity hoarding and interbank market spreads: The role of counterparty risk. Working Paper Series 1126, European Central Bank.

Heijmans, R., Heuver, R., Levallois, C., and van Lelyveld, I. (2014). Dynamic visualization of large transaction networks: the daily dutch overnight money market. Technical report.

Heijmans, R., Heuver, R., and Walraven, D. (2011). Monitoring the unsecured interbank money market using target2 data. DNB Working Papers 276, Netherlands Central Bank, Research Department.

in 't Veld, D., van der Leij, M., , and Hommes, C. (2014). The Formation of a Core Periphery Structure in Heterogeneous Financial Networks. Tinbergen Institute Discussion Papers 14-098/II, Tinbergen Institute.

Iori, G., Masi, G. D., Precup, O. V., Gabbi, G., and Caldarelli, G. (2008). A network analysis of the italian overnight money market. *Journal of Economic Dynamics and Control*, 32(1):259 – 278.

Jackson, M. O. (2008). *Social and Economic Networks*. Princeton University Press, Princeton, NJ, USA.

Judd, K. L. (1998). *Numerical Methods in Economics*. The MIT Press.

Lux, T. and Fricke, D. (2012). Core-Periphery Structure in the Overnight Money Market: Evidence from the e-MID Trading Platform. Kiel Working Papers 1759, Kiel Institute for the World Economy.

May, R. M., Levin, S. A., and Sugihara, G. (2008). Complex systems: Ecology for bankers. *Nature*, 451(7181):893–895.

Rochet, J.-C. and Tirole, J. (1996). Interbank lending and systemic risk. *Journal of Money, Credit and Banking*, 28(4):733–762.

Ruge-Murcia, F. J. (2007). Methods to estimate dynamic stochastic general equilibrium models. *Journal of Economic Dynamics and Control*, 31(8):2599–2636.

Smith, A A, J. (1993). Estimating nonlinear time-series models using simulated vector autoregressions. *Journal of Applied Econometrics*, 8(S):S63–84.

Soramäki, K., Bech, M. L., Arnold, J., Glass, R. J., and Beyeler, W. E. (2007). The topology of interbank payment flows. *Physica A: Statistical Mechanics and its Applications*, 379(1):317–333.

van Lelyveld, I. and in 't Veld, D. (2012). Finding the core: Network structure in interbank markets. Technical report, De Nederlandsche Bank Working Paper No. 348.

Vuillemey, G. and Breton, R. (2014). Endogenous Derivative Networks. Technical report.

Weisbuch, G., Kirman, A., and Herreiner, D. (2000). Market organisation and trading relationships. *The Economic Journal*, pages 411–436.

White, H. (2001). *Asymptotic Theory for Econometricians: Revised Edition* . Academic Press.

A Derivatives in FOC

In equations (9) and (3.6.1) that constitute first-order conditions to banks' approximate optimization problem, we have $\frac{\partial \pi_{i,j,t}}{\partial \tilde{\sigma}^2_{i,j,t}} = \frac{\partial \bar{R}_{i,j,t}}{\partial \tilde{\sigma}^2_{i,j,t}} y_{i,j,t} + \bar{R}_{i,j,t} \frac{\partial y_{i,j,t}}{\partial \tilde{\sigma}^2_{i,j,t}}$ and $\frac{\partial \pi_{i,j,t}}{\partial s_{i,j,t}} = (r - r_{j,i,t}) \frac{\partial y_{j,i,t}}{\partial s_{i,j,t}}$. These derivatives can further be unfolded by the chain rule and the following partial derivatives

$$
\begin{aligned}
&\frac{\partial \phi_{i,j,t}}{\partial m_{i,j,t}} = \beta_\phi, \quad \frac{\partial P_{i,j,t}}{\partial \tilde{\sigma}^2_{i,j,t}} = \frac{\epsilon^2}{(\sigma^2 + \tilde{\sigma}^2_{i,j,t} + \epsilon^2)^2}, \quad \frac{\partial r_{i,j,t}}{\partial \tilde{\sigma}^2_{i,j,t}} = 0.5/\epsilon^2 \\
&\frac{\partial \xi_{i,j,t}}{\partial \phi_{i,j,t}} = \exp(\alpha_\sigma + \gamma_\sigma \log \tilde{\sigma}^2_{i,j,t} + \beta_\sigma \phi_{i,j,t} + \delta_\sigma u_{i,j,t}) \beta_\sigma, \\
&\frac{\partial \xi_{i,j,t}}{\partial \tilde{\sigma}^2_{i,j,t}} = \exp(\alpha_\sigma + \gamma_\sigma \log \tilde{\sigma}^2_{i,j,t} + \beta_\sigma \phi_{i,j,t} + \delta_\sigma u_{i,j,t}) / \tilde{\sigma}^2_{i,j,t}, \\
&\frac{\partial \tilde{R}_{i,j,t}}{\partial \tilde{\sigma}^2_{i,j,t}} = -\frac{\partial P_{i,j,t}}{\partial \tilde{\sigma}^2_{i,j,t}} + \frac{\partial 1 - P_{i,j,t}}{\partial \tilde{\sigma}^2_{i,j,t}} r_{i,j,t} + (1 - P_{i,j,t}) \frac{\partial r_{i,j,t}}{\partial \tilde{\sigma}^2_{i,j,t}} \\
&\frac{\partial y_{i,j,t}}{\partial \tilde{\sigma}^2_{i,j,t}} = C'_{i,j,t} \frac{\beta_I \exp(-\beta_I (r - r_{i,j,t}))}{1 + \exp(-\beta_I (r - r_{i,j,t}))} \left(-\frac{\partial r_{i,j,t}}{\partial \tilde{\sigma}^2_{i,j,t}}\right), \\
&\frac{\partial y_{j,i,t}}{\partial s_{i,j,t}} = C''_{i,j,t} \frac{\beta_\lambda \exp(-\beta_\lambda (s_{i,j,t} - \alpha_\lambda))}{(1 + \exp(-\beta_\lambda (s_{i,j,t} - \alpha_\lambda)))^2}
\end{aligned}
$$

where the logistic function $I_{i,j,t} := \frac{1}{-\beta_I (r - r_{i,j,t})}$ with large scale parameter β_I approximates for the indicator function $\mathbb{I}(r_{i,j,t} \leq r)$. Note that the term $C'_{i,j,t} := \eta_{i,j,t} y_{i,j,t}$ does not depend on monitoring and the term $C''_{i,j,t} := U_{i,j,t} I_{i,j,t} y_{i,j,t}$ does not depend on the search efforts $s_{i,j,t}$.

B Reduced Form, Stationarity and Ergodicity

Substituting the adaptive expectation mechanism in (14) and (15) into the Euler equation for monitoring in (11) and the optimal search strategy in (13) allows us to re-write the full system in reduced form. The reduced form system takes the form of a nonlinear Markov autoregressive process,

$$\mathbf{X}_t = \mathbf{G}_{\boldsymbol{\theta}}(\mathbf{X}_{t-1}, \mathbf{e}_t)$$

where $\mathbf{G}_{\boldsymbol{\theta}}$ is a parametric vector function that depends on the structural model parameter $\boldsymbol{\theta}$, and $\mathbf{X}_t$ is the vector of all state-variables and control variables (observed or unobserved), and $\mathbf{e}_t$ is the vector of shocks driving the system. These shocks are the bank-specific liquidity shocks, the pair-specific shocks to the perception error variance, and the shocks that determine if a link between any two banks is open and trade is possible. Obtaining the reduced form representation is crucial as it allows us to simulate network paths for both state and control variables under a given structural parameter vector. Furthermore, this model formulation allows us to describe conditions for the strict stationarity and ergodicity of the model that are essential for the estimation theory that is outlined in Section 4.

In particular, following Bougerol (1993), we note that under appropriate regularity conditions, the process $\{\mathbf{X}_t\}$ is strictly stationary and ergodic (SE).

LEMMA 1. *For every $\boldsymbol{\theta} \in \Theta$, let $\{\mathbf{e}_t\}_{t\in\mathbb{Z}}$ be an SE sequence and assume there exists a (non-random) $\mathbf{x}$ such that $\mathbb{E}\log^+ \|\mathbf{G}_{\boldsymbol{\theta}}(\mathbf{x}, \mathbf{e}_t) - \mathbf{x}\| < \infty$ and suppose that the following contraction condition holds*

$$\mathbb{E} \ln \sup_{\mathbf{x}' \neq \mathbf{x}''} \frac{\|\mathbf{G}_{\boldsymbol{\theta}}(\mathbf{x}', \mathbf{e}_t) - \mathbf{G}_{\boldsymbol{\theta}}(\mathbf{x}'', \mathbf{e}_t)\|}{\|\mathbf{x}' - \mathbf{x}''\|} < 0 \tag{16}$$

Then the process $\{\mathbf{X}_t(\mathbf{x}_1)\}_{t\in\mathbb{N}}$, initialized at $\mathbf{x}_1$ and defined as

$$\mathbf{X}_1 = \mathbf{x}_1 \quad , \quad \mathbf{X}_t = \mathbf{G}_{\boldsymbol{\theta}}(\mathbf{X}_{t-1}, \mathbf{e}_t) \ \forall \ t \in \mathbb{N}$$

converges e.a.s. to a unique SE solution $\{\mathbf{X}_t\}_{t\in\mathbb{Z}}$ for every $\mathbf{x}_1$, i.e. $\|\mathbf{X}_t(\mathbf{x}_1) - \mathbf{X}_t\| \stackrel{e.a.s.}{\to} 0$ as $t \to \infty$.[17]

The condition that $\mathbb{E}\log^+ \|\mathbf{G}_{\boldsymbol{\theta}}(\mathbf{x}, \mathbf{e}_t) - \mathbf{x}\| < \infty$ can be easily verified for any given distribution for the innovations $\mathbf{e}_t$ and any given shape function $\mathbf{G}_{\boldsymbol{\theta}}$. The contraction condition in (16) is however much harder to verify analytically.

Fortunately, the contraction condition can be re-written as

$$\mathbb{E} \log \sup_{\mathbf{x}} \|\nabla \mathbf{G}_{\boldsymbol{\theta}}(\mathbf{x}, \mathbf{e}_t)\| < 0 \tag{17}$$

where $\nabla\mathbf{G}_{\boldsymbol{\theta}}$ denotes the Jacobian of $\mathbf{G}_{\boldsymbol{\theta}}$ and $\|\cdot\|$ is a norm. By verifying numerically that this inequality holds at every step $\boldsymbol{\theta} \in \Theta$ of the estimation algorithm, one can ensure that the simulation-based estimation procedure has appropriate stochastic properties.

The contraction condition of Bougerol (1993) in (17) states essentially that the maximal Lyapunov exponent must be negative uniformly in $\mathbf{x}$.

[17] A stochastic sequence $\{\xi_t\}$ is said to satisfy $\|\xi_t\| \stackrel{e.a.s.}{\to} 0$ if $\exists\ \gamma > 1$ such that $\gamma^t \|x_t\| \stackrel{a.s.}{\to} 0$.

Definition 1. *The maximal Lyapunov exponent is given by* $\lim_{t\to\infty}\frac{1}{t}\log\max_i \Lambda_{i,t} = \mathbb{E}\log\max_i \Lambda_{i,t}$ *where* $\Lambda_{i,t}$*'s are eigenvalues of the Jacobian matrix* $\nabla\mathbf{G}_{\boldsymbol{\theta}}(\mathbf{x}_t, \mathbf{e}_t)$.

A negative Lyapunov exponent ensures the stability of the network paths. Table 5 uses the Jacobian of the structural dynamic system $\mathbf{G}_{\boldsymbol{\theta}}(\mathbf{x}, \mathbf{e}_t)$ to report numerical calculations of the maximal Lyapunov exponent of our dynamic stochastic network model at the parameters $\boldsymbol{\theta}_0$ and $\hat{\boldsymbol{\theta}}_T$ described in Table 2 of Section 4.3 below. These points in the parameter space corresponds to the starting point for the estimation procedure described in Section 4 and the final estimated point.

Table 5: Lyapunov stability of the dynamic stochastic network model

Parameter vector	$\boldsymbol{\theta}_0$	$\hat{\boldsymbol{\theta}}_T$
Lyapunov exponent	-0.6451	-0.2462

Despite the higher degree of persistence at $\hat{\boldsymbol{\theta}}_T$ compared to $\boldsymbol{\theta}_0$ (higher Lyapunov exponent), the contraction condition is satisfied in both cases as the maximal Lyapunov exponent is negative. This ensures that both $\boldsymbol{\theta}_0$ and $\hat{\boldsymbol{\theta}}_T$ generate stable network paths.

C Network Auxiliary Statistics

In this section we provide formulae for the non-standard auxiliary statistics that characterize specifically the (dynamic) structure of the interbank lending network. First, the global network statistics that relate to the sparsity, reciprocity and stability are given as

$$density_t = \frac{1}{N(N-1)}\sum_{i,j} l_{i,j,t}, \quad reciprocity_t = \frac{\sum_{i,j} l_{i,j,t} l_{j,i,t}}{\sum_{i,j} l_{i,j,t}},$$
$$stability_t = \frac{\sum_{i,j}\left(l_{i,j,t} l_{i,j,t-1} + (1-l_{i,j,t})(1-l_{i,j,t-1})\right)}{N(N-1)}.$$

Further, we maintain information about the *degree distribution*. In the interbank market, the degree centrality of a bank counts the number of different trading partners. For directed networks the out- and in-degree of node i are given by

$$d_{i,t}^{out} = \sum_j l_{i,j,t} \quad \text{and} \quad d_{i,t}^{in} = \sum_j l_{j,i,t}.$$

Instead of considering all $2N$ variables individually, we consider the mean, variance and skewness of the out-degree and in-degree distribution. Note that the mean of degree distribution is proportional to the density. In the estimation procedure we include therefore only the average degree.

The (local) clustering coefficient of node i in a binary unweighted network is given by

$$c_{i,t} = \frac{1/2 \sum_j \sum_h (l_{i,j,t} + l_{j,i,t})(l_{i,h,t} + l_{h,i,t})(l_{j,h,t} + l_{h,j,t})}{d^{tot}_{i,t}(d^{tot}_{i,t} - 1) - 2d^{\leftrightarrow}_{i,t}},$$

where $d^{tot}_{i,t} = d^{in}_{i,t} + d^{out}_{i,t}$ is the total degree and $d^{\leftrightarrow}_{i,t} = \sum_{j \neq i} l_{i,j,t} l_{j,i,t}$, see Fagiolo (2007) for details. We consider the average clustering coefficient which is the mean of the local clustering coefficients.

Second, we compute simple bilateral local network statistics that measure the intensity of a bilateral trading relationship based on a rolling window of size $T_{rw} = 5$ (one week). As a simple measure of bilateral relationships, we compute the number of loans given from bank i to bank j during periods $t' = \{t - T_{rw} + 1, ..., t\}$ and denote this variable by

$$l^{rw}_{i,j,t} = \sum_{t'} l_{i,j,t'},$$

where the sum runs over $t' = \{t - T_{rw} + 1, ..., t\}$. We then consider for each t the correlation between current access and past trading intensity, and between current interest spreads (for granted) loans and past trading intensity,

$$corr(l_{i,j,t}, l^{rw}_{i,j,t}) \text{ and } corr(r_{i,j,t}, l^{rw}_{i,j,t}).$$

All described network statistics are computed for the network of interbank lending at each time period t such that we obtain a sequence of network statistics. We then obtain the unconditional means, variance and/or auto-correlation of these sequences as auxiliary statistics and base the parameter estimations on the values of the auxiliary statistics only.

D Summary statistics of the data

Table 6: Descriptive Statistics of Dutch Interbank Network: The table shows moment statistics for different sequences of network statistics and cross-sectional correlations that characterize the sequence of observed Dutch unsecured interbank lending networks. The statistics are computed on a sample of daily frequency from 1 February 2008 to 30 April 2011.

Statistic	Mean	Std	Autocorr	Skew	Kurtosis
Density	0.0212	0.0068	0.8174	0.8667	3.1983
Reciprocity	0.0819	0.0495	0.2573	0.2903	2.8022
Stability	0.9818	0.0065	0.8309	-0.8590	3.0503
Mean-out-/indegree	1.0380	0.3323	0.8174	0.8667	3.1983
Std-outdegree	1.8406	0.4418	0.6882	0.0553	2.4326
Skew-outdegree	2.8821	1.0346	0.7035	0.6074	2.4572
Mean-indegree	1.0380	0.3323	0.8174	0.8667	3.1983
Std-indegree	1.6001	0.4140	0.6880	0.6997	3.4529
Skew-indegree	2.4030	0.8787	0.6576	0.6714	2.7434
Mean-clustering	0.0308	0.0225	0.4149	0.7900	3.2473
Std-clustering	0.0880	0.0490	0.3587	0.1561	2.7280
Skew-clustering	3.7367	1.5454	0.1213	-0.2213	3.1281
Avg log-volume	4.1173	0.2818	0.4926	-0.2820	2.8220
Std log-volume	1.6896	0.1685	0.3623	0.1541	3.4546
Skew log-volume	-0.3563	0.2818	0.2970	-0.0669	3.2151
Avg rate	0.2860	0.3741	0.9655	1.1044	2.6965
Std rate	0.1066	0.0632	0.7865	1.6668	6.8848
Skew rate	0.6978	1.6399	0.5492	0.6832	2.9469
Corr(r,l^{rw})	-0.0716	0.1573	0.4066	0.0817	2.8539
Corr(l,l^{rw})	0.6439	0.0755	0.4287	-0.7653	4.2833

E Indirect Inference Weights

Following Gourieroux et al. (1993), we adopt a quadratic objective function for indirect inference estimation with diagonal weight matrix based on the optimal weighing matrix that is obtained as the inverse of the covariance matrix of the auxiliary statistics. In particular, we set the criterion function to

$$\hat{\boldsymbol{\theta}}_T := \arg\max_{\boldsymbol{\theta}\in\Theta} \left[\hat{\boldsymbol{\beta}}_T - \frac{1}{S}\sum_{s=1}^{S}\tilde{\boldsymbol{\beta}}_{T,s}(\boldsymbol{\theta})\right]\mathbf{W}_T\left[\hat{\boldsymbol{\beta}}_T - \frac{1}{S}\sum_{s=1}^{S}\tilde{\boldsymbol{\beta}}_{T,s}(\boldsymbol{\theta})\right]',$$

but we use a weight matrix $\mathbf{W}_T$ that differs from the optimal for several reasons. First, the inverse of the covariance matrix is only optimal under an axiom of correct specification. Moreover, even under correct specification the (asymptotically) optimal weighing matrix can lead to larger variance of the estimator in finite samples. Second, for economic theoretic reasons, there are a number of auxiliary statistics that we wish to approximate better than others.

As such we adopt a matrix $\mathbf{W}_T$ corresponding to a an identity matrix, but the weight of the density and $\text{corr}(l_{i,j,t}, l^{rw}_{i,j,t-1})$ is set to 10 and the weight of $\text{corr}(r_{i,j,t}, l^{rw}_{i,j,t-1})$ is set to 50 as we want to match these characteristics particularly well. For computational reasons we minimize the logarithmic transformation of the objective function. For each of the $S = 24$ network paths we burn 1000 periods to minimize dependence on the initial value. The numerical optimization of the objective function is done using a grid search algorithm with multiple starting values.